



D2.3 - DESIGN OF THE PROGRAMMABLE NODES AND MODULAR TRANSCEIVER ARCHITECTURES

Project title	Photonics technologies for ProgrAmmable transmission and switching modular systems based on Scalable Spectrum/space aggregation for future aglle high capacity metrO Networks
Project acronym	PASSION
Grant number	780326
Funding scheme	Research and Innovation Action - RIA
Project call	H2020-ICT-30-2017 Photonics KET 2017 Scope i. Application driven core photonic technology developments
Work Package	WP2
Lead Partner	CTTC
Contributing Partner(s)	POLIMI, TUE, VTT, VERT, SMO, TID, EFP
Nature	R(report)
Dissemination level	PU (Public)
Contractual delivery date	31/03/2020 (extended to 31/07/2020)
Actual delivery date	30/07/2020
Version	1.1

History of changes

Version	Date	Comments	Main Authors
0.0	30/04/2020	ToC	Michela Svaluto Moreolo, Ricardo Martínez
0.1	14/07/2020	First integrated version	Michela Svaluto Moreolo, Ricardo Martínez, Javier Vilchez, Laia Nadal, Raul Muñoz, Josep M. Fabrega, Josep Mangués, Paola





			Parolari, Mariangela Rapisarda, Alberto Gatto, Pierpaolo Boffi, David Larrabeiti, Juan P. Fernández Palacios, Gabriel Otero, Pedro Reviriego, Victor López, Jose D. Martínez, Jose A. Hernandez, Oscar González, Netsanet Tessema, Ripalta Stabile, Nicola Calabretta, Christian Neumeyr, Roland Heuvelmans
0.2	20/07/2020	Second integrated and revised version	Michela Svaluto Moreolo, Giorgio Parladori, Raffaele Corsini, Germano Gasparini, Paola Parolari, David Larrabeiti, Juan P. Fernández Palacios, Giovanni Delrosso
0.3	20/07/2020	Revised version including quality review	Netsanet Tessema, Nicola Calabretta, Michela Svaluto Moreolo
1.0	27/07/2020	Final check	Paola Parolari, Pierpaolo Boffi
1.1	30/07/2020	Final version	Michela Svaluto Moreolo



Disclaimer

This document contains confidential information in the form of the PASSION project findings, work and products and its use is strictly regulated by the PASSION Consortium Agreement and by Contract no. 780326.

Neither the PASSION Consortium nor any of its officers, employees or agents shall be responsible or liable in negligence or otherwise howsoever in respect of any inaccuracy or omission herein.

The contents of this document are the sole responsibility of the PASSION consortium and can in no way be taken to reflect the views of the European Union.



This project has received funding from the European Union's Horizon 2020 Research and Innovation Programme under Grant Agreement No 780326.



Table of contents

Executive Summary	6
1 Introduction	7
2 PASSION programmable modular system architecture design	8
2.1 Target use cases and network path analysis	9
2.1.1 Summary of target use cases.....	9
2.1.2 Use case #6: 5G C-RAN support	11
2.1.3 Network path analysis toward supporting HL4-HL1/2 all-optical paths	14
2.2 Programmable modular system architecture design	17
3 PASSION switching and aggregation node architectures	19
3.1 HL1/2, HL3 nodes.....	20
3.2 HL4 nodes	21
3.3 Advances in PASSION node elements	21
3.3.1 Photonic switch	21
3.3.2 Add/drop wavelength selective switch (WSS)	21
3.3.3 Multicast switch (MCS).....	22
3.4 Control aspects of switching node.....	22
4 PASSION transceiver architecture	23
4.1 S-BVT architecture	23
4.1.1 PASSION Transmitter architecture	24
4.1.2 PASSION Receiver architecture	29
4.2 Modularity and Programmability	32
5 Optical transmission analysis and feasibility study	35
5.1 Optical impairment tolerance.....	35
5.1.1 E/O impairments transmitter side	36
5.1.2 E/O impairments receiver side	36
5.1.3 Multi-channel transmission.....	37
5.2 Feasibility study	38
5.2.1 Analysis of sample connections based on MS4 network architecture definition	38
5.2.2 NL analysis of worst cases.....	39
5.2.3 PASSION photonic system architecture assessment for multi-hop HL4-HL2/1 connectivity enabling IP-offloading	43
5.2.4 OSNR requirements for the support of 90% HL4-HL2/1 primary and secondary paths	44
6 Conclusions	47
7 References	49
8 Acronyms.....	51







EXECUTIVE SUMMARY

This report corresponds to the deliverable D2.3 of PASSION project, providing the design of the programmable nodes and modular transceiver architectures, targeted within the PASSION project to address the need of future high capacity and agile metropolitan networks, that will be then integrated, validated and demonstrated within the WP5 context.

The purpose of this deliverable is to provide a consolidated architecture of the PASSION network elements based on the first, preliminary definition of the key system elements included in MS6, in view of their integration and proof of concept validation within WP5. This document describes and details the different node and transceiver architectures defined in T2.3. Furthermore, the PASSION modular approach and modularity options/choices for the proposed photonic technology solutions are defined and analysed, targeting multi-Tb/s connectivity and identifying the programmable parameters of the system and subsystems, for a dynamic system adaptation to the need of a flexible metro network. The most challenging use cases and suitable applications are identified and taken into account for the proposed architectures design and feasibility study. The network requirements and programmability aspects have been considered as defined in D2.2, while taking into account the technology advancements in the framework of WP3 and WP4, and the related features and constraints.

The main elements and component functionalities of the optical switching node are described, specifying the architecture according to the different hierarchical levels (HLs). The transceiver architecture is also provided, focusing on the modular approach for the transmitter and the receiver design, the adopted technologies and target capacities, also based on the identified HLs and node type, functionalities and granularities. Based on the identified use cases and for addressing the challenges of future large, dynamic and agile (5G-supportive) MANs, feasibility studies have been conducted and are here reported. Numerical analysis of different transmission impairments, using an improved PASSION simulation tool, and the results of extensive simulations are included in this report. Furthermore, with also the feedback of experimental assessment of the PASSION concept performed within WP5 and a theoretical model as a benchmark, important observations are derived for the architecture design and optimization, showing that promising results are expected for the implementation of the targeted PASSION solution.

Further refinement/optimization of the final node and transceiver architecture design can be performed within WP2, based on next advances on the work developed within WP3, WP4 and with further feedback of the activities performed within WP5.

1 INTRODUCTION

Future high capacity and agile metropolitan area networks (MANs) pose several challenges to the technological solutions to be developed, in order to address the connectivity requirements and dynamic bandwidth allocation with reduced cost, power consumption and footprint, expected in this network segment. The design of a programmable modular system comprising suitable optical switching nodes for agile spectrum/space aggregation and sliceable bandwidth/bitrate variable transceiver (S-BVT) architectures is key to enable dynamic connectivity and multi-terabit capacity networking.

The PASSION modular system is designed by taking into account i) the considered use cases and network architecture requirements (described and discussed in D2.1 and D2.2); ii) the technological solutions and developments of WP3 and WP4; iii) the programmability and control aspects defined in D2.2.

In this document (Section 2), the identified use cases are briefly reported with special focus on the cost-effective ultra-broadband transport and expansion in a large MAN, targeting a feasible pay-as-you-grow scheme and dynamic capacity adaptation. Special attention is devoted to the case enabling IP offloading of hierarchical level (HL) 3 traffic, identified as the most challenging for the support of high capacity connectivity from HL4 (first level of aggregation) to HL2/1 at the core of the metro network. The targeted use cases (and particularly the worst case) identification and analysis is crucial for estimating the suitability and applicability of the proposed PASSION concept and solutions. Furthermore, the case of 5G C-RAN support for midhaul/fronthaul traffic transport over the MAN is also described as another suitable application of PASSION system solutions.

Then, the PASSION programmable system architecture is described encompassing the two main elements, which are the optical switching node and the S-BVT. According to the target very large MAN and its hierarchical level structure (see Figure 1), the PASSION switching node and transceiver architectures as well as their modularity, functionalities and capabilities are defined.

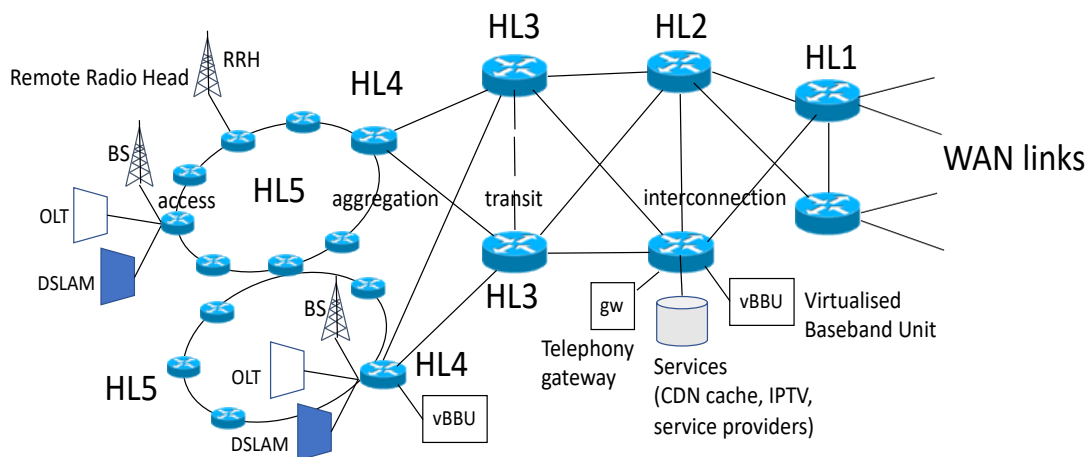


Figure 1. Schematic IP Layer hierarchy of routers as defined in [D2.1]

As detailed in Section 3, the PASSION node elements, architectures and functionalities are suitably defined, designed and implemented according to the specific HL. In particular, for low hierarchy level HL4 node, a simpler and cost-effective design is envisioned; while for high hierarchy levels (node architecture for HL1/2 and HL3 nodes) more advanced switching and aggregation node architectures are defined able to efficiently manage both the spectral (with finer granularity) and spatial



dimensions. The main advances in PASSION elements composing the node (performed in WP3 and WP4) allow to consolidate the design of the photonic switch, the add/drop wavelength selective switch (WSS), and the multicast switch (MCS), to handle express traffic, added traffic and dropped traffic. Accordingly, the programmability and control aspects of the switching nodes are specifically defined. In particular, at HL3 and HL2/1 nodes spectral and spatial aggregation can be implemented to enable specific advanced functionalities targeting high level of flexibility, minimizing the complexity and efficiently utilizing the resources. Furthermore, the envisioned flexible and modular design results in a scalable architecture enabling capacity upgrade.

Section 4 describes the S-BVT architecture specifying the transmitter and receiver subsystems design, according to the advances in WP3 and WP4 technology and solutions, considering network requirements and use cases, as well as programmability aspects (according to D2.2). The PASSION S-BVT is also designed to be modular and ease capacity enhancement and adaptation as well as an efficient resource usage to address the challenges of future MANs. The modules composing the transceiver enable the generation of multiple flows with sub- and super-wavelength granularity exploiting multicarrier modulation and PASSION technologies adopting direct modulated vertical cavity surface emitting lasers (VCSELs), photonic integration and coherent detection. The integrated fundamental module enables up to 2Tb/s, while up to 8Tb/s can be achieved with a fully equipped (in the spectral dimension) transceiver. Above 100Tb/s can be supported by exploiting the polarization and spatial dimensions. Similarly, to the node architecture, simple S-BVT architecture (fundamental module) is envisioned for HL4 nodes, while fully equipped exploiting multiple dimensions are considered to equip higher level nodes.

Section 5 deals with optical transmission analysis and feasibility study to identify the impairment tolerance of the proposed solution and optimizing it accordingly. Specifically, both the transmitter and receiver sides are considered towards achieving the targeted performance, as well as the system architecture elements enabling the aggregation of multiple data flows to address the target capacities according to the network requirements. The multi-channel transmission is analyzed, in order to prevent crosstalk effect. Furthermore, the analysis of sample connections based on the network architecture definition in D2.2 with the traversing of specific node elements/architectures, as well as non-linear analysis of the worst cases are discussed in line with the path analysis and characterization. As the case of IP offloading is considered one of the most challenging, the PASSION photonic system architecture assessment for multi-hop HL4-HL2/1 connectivity is reported and discussed also including an analysis of the optical signal to noise ratio (OSNR) requirements for the support of HL4-HL2 primary and secondary paths.

2 PASSION PROGRAMMABLE MODULAR SYSTEM ARCHITECTURE DESIGN

This section is devoted to briefly reviewing the PASSION use cases and requirements, focusing on the most challenging use case analysis, including latest table and results of the path analysis and characterization. The case of 5G C-RAN support for midhaul/fronthaul traffic transport over the MAN is also detailed as another PASSION system solutions application. Also, the section reviews the overall PASSION programmable modular system, suitably designed for an optimal use of the available metro network resources.



2.1 TARGET USE CASES AND NETWORK PATH ANALYSIS

PASSION’s development approach is use-case driven. That means that the design cycle takes into account a preliminary set of use cases to extract requirements for PASSION technology (deliverable D2.1 [D2.1]), and keeps on studying additional use cases during the project lifetime to be considered in WP2’s final deliverable D2.4, where an in-depth techno-economic analysis based on the most relevant use cases will be performed. On this direction, in D2.2 [D2.2], use case #6 *C-RAN support* was appended to the use case list of scenarios where to exploit PASSION.

In this section, for the sake of self-containment, we reproduce the list of use cases in subsection 2.1.1, and we develop the description of use case #6 in section 2.1.2. Then, in section 2.1.3 we expand in several aspects the description of use cases #3, as very challenging and relevant use case for future agile MANs and for the application of PASSION technologies and solutions.

2.1.1 Summary of target use cases

The following table enumerates the target use cases and identifies their requirements.

Summary of targeted use cases and further refinement use case #6 C-RAN support [Lar20].

Table 1 Summary of target use cases and their main requirements from [D2.2]

Use Case #	Use Case Descriptor	Main requirements
#1	Cost-effective ultra-broadband transport and expansion in a large MAN. Key pursued objective is to provide a feasible ‘ pay as you grow ’ scheme	<ul style="list-style-type: none"> • High transport capacities • High modularity featuring “pay as you grow”: 2Tb/s – 16Tb/s • Granularity of data rate allocation at 50Gb/s, supporting heterogenous data rate demands: 50, 100, 150 and 200 Gb/s • SDN-based programmability of network elements and devices • HL1/2 nodes equipped with interfaces supporting aggregate capabilities of tens of Tb/s • Cost-effective upgradeable optical transceivers for HL4 starting at 1 or 2 Tb/s. • Sliceability of transceivers to support simultaneous multiple connections stemming from a single device. • Fast on-line routing and spectrum assignment (RSA) algorithms to attain efficient resource utilization.
#2	Embedded support of on-line restoration mechanisms to fast recover disrupted services caused by link and node failures (this is a compulsory reliability-by-design feature included use case #1)	<ul style="list-style-type: none"> • Ability to compute and program backup (link and node disjoint) paths restoring “on the fly” disrupted services. • Backup paths may allocate the same VCSELS (i.e., optical carriers / central frequencies) as the primary paths at the endpoints if so required. • Make-before-break and Break-before-make approaches are to be studied determining the implications within the SDN control interfaces and functions • Evaluation under both dynamic traffic scenario along with link failure generation.



		<ul style="list-style-type: none"> • Connection requests demanding heterogeneous data rates with 50Gb/s granularity • Multiple performance indicators: blocked bandwidth ratio, restorability, average setup time, etc.
#3	Cost-effective ultra-broadband transport and expansion in a large MAN: Dynamic capacity adaptation and HL3 IP off-loading	<ul style="list-style-type: none"> • Support of all-optical HL4-HL2/1 paths. • Ability to perform packet (IP) off-loading of HL3 traffic onto the optical layer, leveraging S-BVT and control plane capability to set up direct HL4-HL1 optical channels. • Low-penalty optical switching and multiplexing capability of the PASSION HL4 and HL3 switches to enable long-distance multi-hop all optical circuits without electronic regeneration. • Multi-layer SDN control integrating real-time knowledge of packet (IP) network usage as well optical network domain. The aim is to leverage the best of both the optical and the service layer, in order to make the most efficient use of all the network resources (packet ports, optical spectrum, transceivers, etc.) • Fast multi-channel provisioning and reconfiguration (in the order of minutes in final production devices) to better adapt to traffic changes variability during a day. • Devising routing and wavelength/spectrum assignment RWA/RSA algorithms to attain efficient resource selection leading to low blocking probabilities even for high traffic loads. • Programmability of traffic trunks and optical circuits to daily patterns. • Sliceability should make it possible to simultaneously connect HL4 to HL2/1 nodes and locally connect neighboring HL4 nodes.
#4	Interconnection for distributed computation sites (e.g., CDN) within the MAN: efficient protection schemes	<ul style="list-style-type: none"> • Ability to automatically migrate a full edge CDN node to another backup location (2 Tb/s) • Agile switch-over and switch-back capabilities handled by a centralized SDN controller • Fast multi-channel (re-)configuration (in the order of seconds in production products) when applying a switch-over/switch-back or over-flow of traffic to another data center • Full control of end-to-end latencies to keep the requirements of the services being accommodated
#5	Support of massive events: drastic dynamic re-allocation of capacity near the access	<ul style="list-style-type: none"> • Capability to dynamically allocate massive transport capacity at an HL4 node to support eventual concentration of people demanding high consuming data traffic services and applications such as augmented reality (2Tb/s) • Network elasticity to re-use that capacity after the event in the aggregation segment.



This approach has been used in some LTE-A deployments, where fiber is available for 20MHz channels, but the transport of fronthaul has become much more challenging for 5G new radio. In December 2017, 3GPP published TS38.1047 Release 15 as the specification of the New Radio air interface for 5G. This technical specification defined two frequency ranges: FR1 (under 6 GHz) with component bandwidths ranging 5-100 MHz and sub-carrier spacings 15/30/60 KHz; and FR2 (24-86 GHz) with component bandwidths ranging 50-400 MHz, and sub-carrier spacings 60/120 KHz. In addition, 8 possible functional split options were further defined in TR38.801 as depicted in Figure 1. This generates a wide range of fronthaul traffic patterns. However, the most relevant split options are Option 2 (F1 interface that processes up to RLC (Radio Link Control) layer) and Option 7 (intra-PHY, being option 7-2 equivalent to eCPRI split I_U=II_D). In split option 7, the Low PHY box performs the removal of the cyclic prefix, FFT and Resource Block de-mapping in the uplink (split I_U in eCPRI), and modulation, layer mapping and precoding in the downlink (split II_D in eCPRI). This leads to a traffic volume that is proportional to the user traffic in the cell. However, for a stable utilisation η the traffic can be assumed to produce a deterministic fronthaul pattern given by:

$$R_{\text{Split } I_U} = N_{sc} \cdot U_{sc} \cdot \eta \cdot T_s^{-1} \cdot 2 \cdot N_{\text{bits}} \cdot N_{\text{ant}}$$

Where N_{sc} is the number of subcarriers, U_{sc} is the percentage of usable subcarriers (not used as guard bands), η the utilisation, N_{bits} is the amount of bits per samples and N_{ant} the number of antenna elements, where we assume that the number of active MIMO layers matches the number of antennas of the gNB. Table 2 provides sample rate and burst sizes for split I_U traffic with 5G New Radio numerology assuming $\eta=100\%$ utilisation, usable subcarriers $U_{sc}=95\%$, $N_{\text{bits}}=15$ bits/sample.

Table 2 Rate and burst size for split IU traffic with 5G New Radio Numerology for 100% Utilisation

B [MHz]	Δf [KHz]	N_{sc}	T_s [μs]	#Antennas or max MIMO layers	R [Gbps] per RF Channel	Burst Size (bytes)
20	15	1267	66.7	2	1.14	9503
50	15	3167	66.7	2	2.85	23753
100	60	1584	16.7	32	91.24	190080
100	60	1584	16.7	256	729.91	1520640
200	120	1584	8.3	32	182.48	190080
200	120	1584	8.3	256	1459.81	1520640
400	120	3167	8.3	32	364.84	380040
400	120	3167	8.3	256	2918.71	3040320

As it can be seen, the impact of mm-wave with broader radio channels (400Mhz) and the use of massive MIMO as the way to circumvent the challenge of using high frequencies, has a multiplicative effect that may lead to rates of up to 3 Tb/s. This means very high rates for the numerology of 5G new radio that can justify the use of PASSION technology.

The burst sizes, if we consider its transport over packet switching technologies, are challenging too. As described, the Evolved Universal Terrestrial Radio Access (E-UTRA) specifications 3GPP TS 36.211 and the New Radio (NR) access technology for 5G 3GPP TS 38.211 make use of Orthogonal Frequency Division Multiplexing (OFDM). The specifications define the time intervals for data transmission based on the OFDM symbol time, which is the smallest E-UTRA or NR frame with a meaning. This frame becomes a large burst of data (as big as 3MB according to our table for 400MHz and 256 antenna elements) to be transmitted over a burst of packets.

The transport of new radio traffic to be processed deep into the MAN in a centralized way (in order to achieve high degree of sharing of radio processors) is further complicated by the real time



transport and synchronisation requirements of this traffic. On the one hand, there is a 100µs deadline to deliver signals for MAC processing, set by IEEE 802.1CM and eCPRI, which is due to the HARQ timers of the retransmission scheme of LTE and 5G. On the other hand, the evolution of the air interface requires processing coming not just from one centralised MIMO antenna array, but the combination of signals from antennas scattered over a large area. The following figures try to illustrate this evolution. Figure 3 shows a C-RAN deployment for 5G. The processing at the DU may imply the synchronisation of one or two flows, if CoMP-JT (coordinated multipoint with joint transmission) is used to deal with inter-cell interference and increase transmission capacity.

Regarding latency, option 2 requires 1.5 ms – 10 ms, while option 7 (Intra-PHY) - eCPRI Split 1_u has a network latency budget of 100 µs.

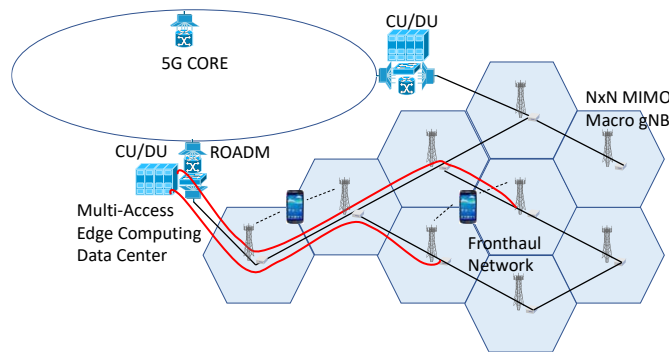


Figure 3 Macro-cell based fronthaul network

If the densification process follows the small cell approach or the cell-free approach, the amount of flows that need to be synchronized and the requests for synchronization will arrive more frequently than in 4G, given that the user equipment (UE) may associate to a macro gNB and a couple of small cells within, in order to perform soft handovers between them or make use of 5G capability to aggregate the transmission capacity of many radio links simultaneously (Figure 4).

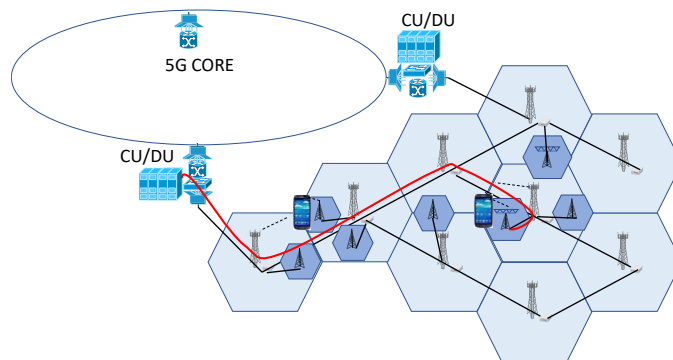


Figure 4. Small-cell-based fronthaul network densification

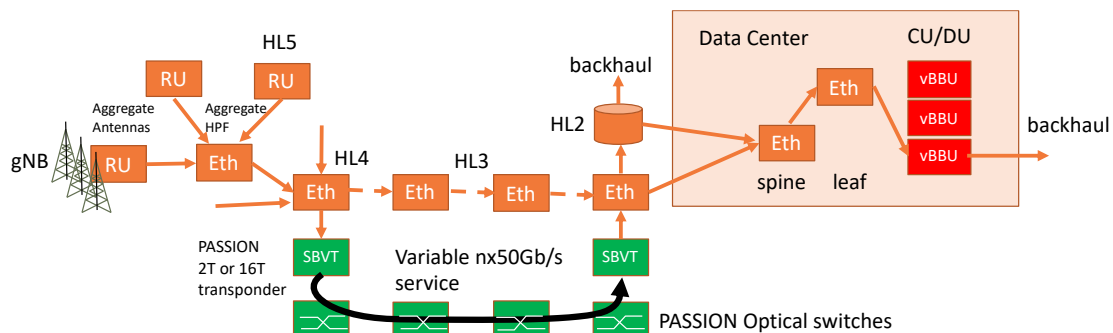




Figure 5. PASSION architecture proposed to support High400 and HL3 off-loading.

In this scenario, S-BVTs may be used as a flexible alternative to Ethernet transceivers pluggable to routers and/or Ethernet switches [Lar20]. PASSION architecture shows a number of advantages over fixed Ethernet transceivers and switches like: a) the possibility to configure a flexible rate; b) the capability to set up circuits to many endpoints simultaneously (this makes it possible to distribute traffic to different switches and configure protection schemes with a single transceiver); c) the potential to be adapted to work in the access (out of the scope of this project) and hence support High100 (100µs) and High25 (100µs) fronthaul [802.3CMde]; d) the potential to create low jitter circuits as an alternative to multi-hop Ethernet packet queuing (Figure 5); e) the capability to support jumbo frames (in Ethernet, the practical frame size is limited to 2000 bytes for backward compatibility) that may match the size of fronthaul OFDM symbol bursts (the jitter induced by segmented transport is extremely relevant); f) the ability to use only the wavelengths necessary to carry the traffic of that end point; g) an SDN-based control plane able to support smart networking suitably configuring the network elements according to the traffic need and finally h) a capacity greater than Ethernet to carry 5G new radio and beyond 5G.

2.1.3 Network path analysis toward supporting HL4-HL1/2 all-optical paths

Both use cases #3 and #6 have a challenging goal from the transmission/switching perspective: the setup of all-optical paths from any HL4 (a node that aggregates traffic from the access HL5 nodes) to the closest HL2 or HL1 nodes (MAN core). As described in D2.2, two types of paths are studied: primary paths, and secondary paths used for protection of primary paths. Secondary paths are physically disjoint to the primary one and are setup from the HL4 under consideration to hierarchical level HL1/2. Thus, they may terminate at a different HL1/2 node than the primary path. Logically, secondary paths are longer than primary paths [D2.1].

A quick analysis reveals that, given the typical link lengths of the reference topology and the switching impairments, a better OSNR is obtained if the metric employed to calculate the shortest path is the number of hops rather than the link length. The following table provides a statistical characterization of primary and secondary paths, when this metric is used.

Table 3. statistics of primary and secondary paths HL4-HL1/2, computed as the shortest according to number of hops

HL4-HL1/2 path type	Mean/Median (km)	Mean/Median (hops)	Std (σ) (km)	Std (σ) (hops)	90% percentile (km)	90% percentile (hops)	Max (km)	Max (hops)
Primary	36.14/30.5	4.19/4	25.19	1.39	68.42	6	131.3	8
Secondary	74.7/72.7	7.6/7	29.45	2.17	115.20	11	148.4	14

The 90-percentiles were computed directly on the computed path sets, suggesting that the assumption of a normal distribution of distances to estimate any other percentile from the mean and standard deviation is conservative in our reference network. In particular, the 90%-percentile in number of hops is 6 for the primary paths, whereas the standard distribution would give 6 as 68%-percentile.

If instead of the hop-count metric we use the physical length metric, the 90%-percentile distance is reduced to 56.96km, but the 90%-percentile number of hops becomes 13 >> 6, which proves that minimizing hops is more convenient as a starting point to find the best OSNR path. Same 90-percentile values for secondary paths are 94km and 25 hops, which also corroborate this assertion.





As mentioned, all these statistics characterize the distance between any HL4 node to the closest HL2 or HL1 node, which seems to be enough as a practical target for all optical end-to-end connectivity. This is because most of the traffic is aggregated towards the core and once in the top of the hierarchy the traffic is disaggregated to reach the right HL2 or HL1 hosting the target service (typically CDN (HL2) or Internet WAN connectivity (HL1)). This disaggregation can take place at the IP layer of HL2, and then intra-HL1/2 traffic transport can happen over a simple mesh of high capacity HL2/HL1 circuits. Otherwise the amount of circuits that an HL2/HL1 needs to deal with explodes, as it has to terminate not just the circuits coming from all HL4 hierarchically dependent on it but the circuits coming from any HL4 of the network.

However, an operator may also like to address the more challenging any-HL4 to any-HL2/1 all optical connections and PASSION would like to assess this case as well. In particular, in section 5.2.2 the worst-case paths for any-HL4 to any-HL2/1 in our reference network will be assessed (Figure 6).

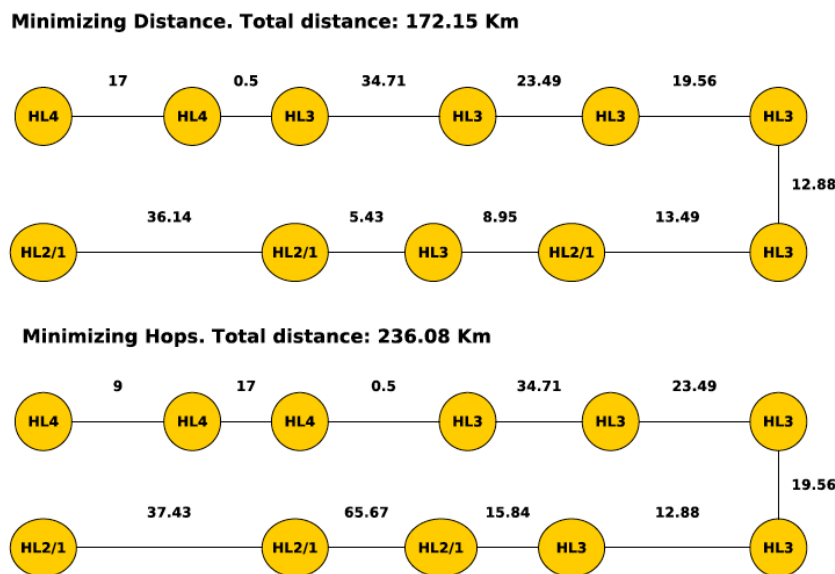


Figure 6. Worst case paths in the PASSION reference network topology for any-HL4 to any-HL2/1 connectivity.

In order to assess the viability of a path for PASSION, we need to consider the impairments of the following network elements on the end-to-end OSNR:

- Optical fiber
- Optical Amplifiers (OA)
- PASSION nodes: two types of optical switches or ROADMs have been proposed in PASSION: HL1/2 and HL3, and HL4 with different capabilities and insertion impairments, as mentioned in D2.2 and explained with more detailed in this document in the next section.

As detailed in Sec. 5, the impairments caused by PASSION nodes are modelled through a simulation tool endorsed by experimental measurements. Regarding optical amplification and fiber transmission, the linear model has been used. Since the location of the amplifiers needs to be determined, we shall make the following considerations:

- A link may be traversed by paths of multiple arbitrary lengths, so the optimal location of OA for a path may not be optimal for another path. A global optimal placement of OAs for a set of paths that minimizes the total cost would change if the set of paths changes. Therefore, in





general the operator will use uniform rules rather than base OA placement on the implementation of individual paths.

- Operators prefer to minimize the amount of OA and their cost, thus: (a) Maximum span length between ILA (In-Line Amplifiers) is preferred to shorter span options (65km over 40km, 20km, etc), (b) node amplification is preferred to amplification on the outside plant because the OPEX of outdoors ILA is higher. However, the QoT (quality of transmission) may be improved by using shorter amplification spans.
- 100% of links in our reference topology are shorter than 65km long. Thus, in principle, they all can be supported without ILA.

. For links > 65km and for those designs that include ILAs every S kms there are two options:

- Every S km, calculating the spans length backwards from the HL node to the previous. For example: for a link length of 140Km and S=65: $140/65 = 2.154 \Rightarrow 2$ spans of 65km and one span of $0.154 * 65 = 10$ km. This is the approach used in the simulations of Section 5.
- Equally-spaced. For the same example of 140Km, the span lengths would be 46.6km.

As a conclusion, we shall assume that every HL3 or HL4 node has an OA for each incoming fiber irrespective of the link length and, as an option, the network designer may decide to use ILAs every S km to improve the QoT.

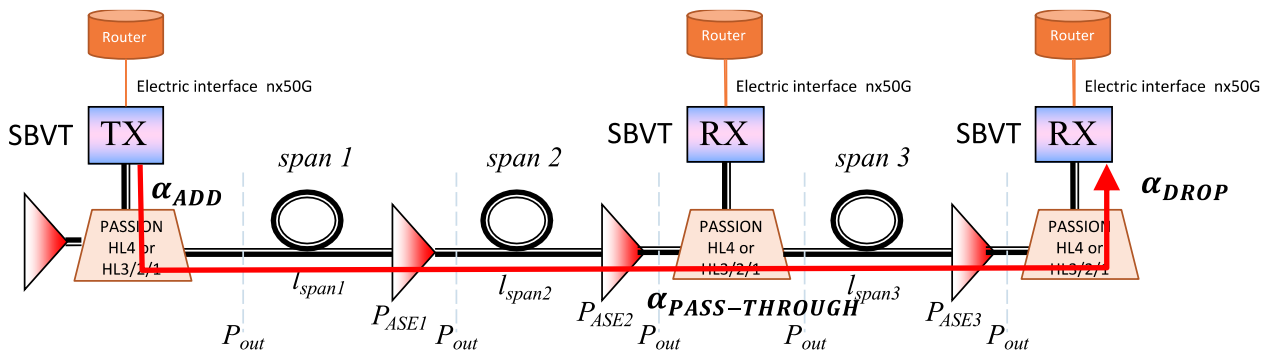


Figure 7 Example of 2-hop all optical path and location of Optical Amplifiers

In order to analyze the goodness of PASSION technology when it comes to supporting the all-optical paths required by use cases #3 and #6, we propose to estimate by simulation the percentage of HL4-HL2/1 paths that can be set up and used all optically in PASSION's reference topology, and determine their maximum feasible rate per wavelength among three configurable settings: 25G, 40G and 50G. The paths that do not support at least 25G, will be regarded as non-feasible and will require an intermediate electronic regeneration stage (e.g. an IP HL3 router). In order to obtain these simulations due to computing complexity of NLSE (nonlinear Schrödinger equation) based methods we use a multichannel co-polarized linear method which features all the linear characteristics of the network elements. A detailed description of the method and a comparison with results obtained in the nonlinear (NL) regime can be found in Sections 5.1.3 and 5.2.4.

To perform this study, a very high-level perspective of the proposed methodology to be applied in D2.4 and in the network design support tools of D6.7 is defined in Table 1. It should be considered that, as it will be seen in Section 5, the OSNR does not necessarily vary monotonously with the number of traversed nodes. Therefore, for convenience, the easily predictable impairment effects





(fiber and OAs) have been separated from the complex simulation-based ones (cascaded node traversal) so that the simulation results can be re-used for any path length.

Table 4. Overall methodology to assess the support of all-optical HL4-HL2/1 paths by PASSION

Step	Description	Comment
Step 0	In advance, by simulation, compute a set of arrays of minimum end-to-end OSNR required to traverse x HL4 nodes and y HL3/HL2/HL1, for each target rate: 25G, 40G, 50G. These OSNR budgets correspond to fiber and optical amplifiers alone, after the effect of node traversal has been simulated.	It should be recalled that two type of optical nodes are available in the PASSION architecture: HL4 or HL3=HL2=HL1
Step 1	Take as input a topology under study. For each HL4 node: compute the primary path to HL2/1 using Dijkstra's algorithm with the number of hops as metric to obtain a candidate.	The best-OSNR path is likely to be this path or a variant of it.
	Apply a heuristic search around this candidate path using the path evaluation method described in Section 5:	E.g. deleting randomly links or nodes from the topology.
	1. Determine the minimum OSNR required by the path, according to the number of HL4 and HL3/2/1 contained in the path by checking the tables computed in Step 0.	
	2. Apply the multi-span transmission linear model to calculate the OSNR of the path and check on each table if the corresponding threshold is passed.	The ones that are over the thresholds set by the tables of step 0.
Step 2	After computing the best OSNR primary path, remove the links and nodes of this path from the topology and compute the best OSNR secondary path by using the same procedure of Step 1 on the new topology.	
Step 3	Compute the statistical distribution of supported rates among all computed primary and secondary paths.	A fraction of these paths is expected to be classified as non-feasible.

As discussed, a complete description of the method to carry out the analysis of individual paths is reported in Section 5.

2.2 PROGRAMMABLE MODULAR SYSTEM ARCHITECTURE DESIGN

The PASSION programmable system architecture is based on two main elements: the optical switching node and the S-BVT, including the photonic transmitter (S-BVT Tx) and the coherent receiver (CO-Rx) module (CRM).

The system architecture has been carefully designed to target the envisioned use cases and requirements in terms of capacity and paths to be supported. Furthermore, the proposed solution should also target low power consumption and footprint. This is accomplished with the adoption of the technologies developed in WP3 and WP4, which are taken into account for a suitable and efficient architecture design.

The modularity is a key feature for the node and transceiver composition and scalability, according to the pay-as-you-grow model and/or license-based element activation, in view of the network





expansion/upgrade. Thus, the system or a specific node/transceiver can grow-as-needed to achieve the target capacity/flexibility, also according to the evolution of the network. Further details on the modularity choice for the PASSION network elements (node, S-BVT and related subsystems) are provided in Sec. 3 or Sec. 4, respectively.

Programmability also is a key feature to accomplish the required flexibility, dynamicity and adaptation to the available resources and requested traffic demands. Both spectral and spatial resources should be efficiently managed to comply with the stringent requirements, in terms of capital and operational expenditures (CAPEX/OPEX) imposed by MANs.

The programmable optical system enabling spectrum and space aggregation/switching, envisioned within the PASSION project to target the requirements of future MANs, is illustrated in Figure 8. The network nodes are equipped with modular S-BVTs and each network element is configured by a software defined networking (SDN) controller, by means of dedicated control agents. Modularity allows enhancing the capacity and features according to the need. Thus, the S-BVT and nodes are suitably designed/sized according to the metro network node type or hierarchy/aggregation level, as will be explained with more detail in Sec. 3 and Sec. 4. Particularly, lower level metro-aggregation nodes (HL4, aggregating traffic from edge nodes at HL5) are equipped with simple and cost-effective transceiver and switching elements exploiting only the spectral dimension. The fundamental module with an integrated design enables to support up to 2Tb/s. Higher level metro-core nodes (HL2/1) adopt fully equipped (with modular approach) transceivers and photonic switching nodes supporting multiple functionalities and granularities, handling both spectral and spatial dimensions. The fully equipped S-BVT based on the 2Tb/s fundamental module enables to support up to 8Tb/s, fully exploiting the spectral dimension, and beyond (>100Tb/s) when adopting also the polarization and spatial dimensions.

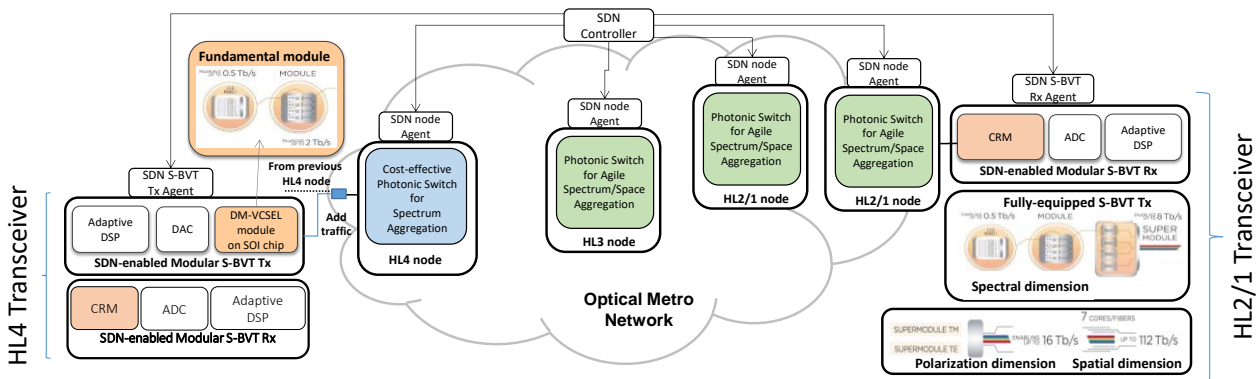


Figure 8. Schematic of PASSION programmable system architecture.

The multiple modules at the transmitter (Tx) side of the S-BVT consists of direct modulated (DM) VCSELs characterized by large bandwidth ($\geq 18\text{GHz}$). The fundamental building block is a silicon-on-insulator (SOI) chip integrating multiple VCSELs at operating wavelengths within the C-band to efficiently exploit the spectral resource. The generated flows are aggregated/disaggregated and switched in the spectrum and space dimensions at the PASSION node, according to the node architecture. The dropped traffic is finally recovered at the receiver (Rx) side of the S-BVT by means of multiple coherent receiver (CO-Rx) modules integrated on PIC. The adaptive digital signal processing (DSP) at the Tx and Rx allows to suitably adapt the multiple data flows to the required bandwidth, traffic demand and QoT required by the established connection. In particular, by exploiting multicarrier modulation (MCM), variable bandwidth/bitrate adaptation (per flow) with sub-wavelength granularity is enabled [Sva16].



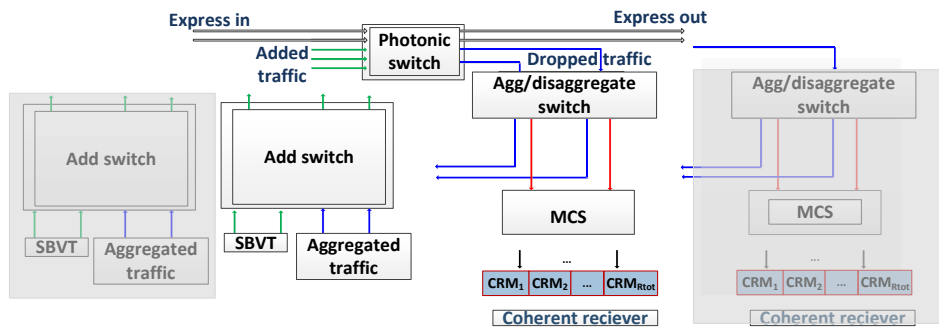


To fully integrate the programmability and softwarization in the optical system and exploit their inherited advantages, it is crucial considering the peculiarities of the elements and devices to be configured, as well as the limitations/potentialities of the adopted photonic technologies. This also implies carefully identifying the parameters that can be accessible/programmable and involves defining the information model that will be used by the SDN controller.

Programmability and control aspects are briefly discussed in this document, with special emphasis on programmable parameters. Further details on these aspects related to the PASSION approach and network architecture have been defined and are reported in D2.2 [D2.2].

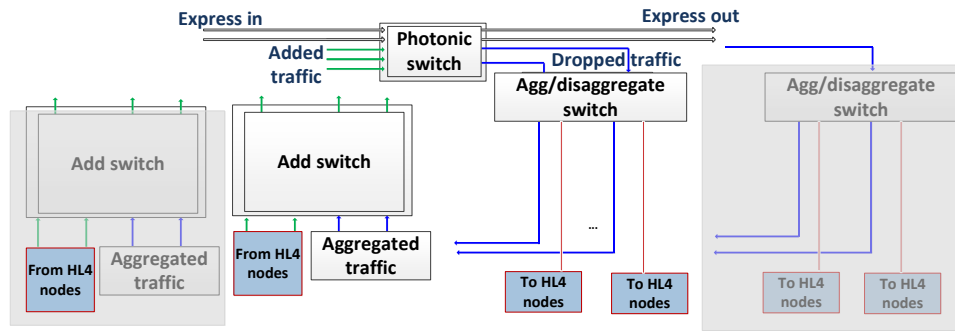
3 PASSION SWITCHING AND AGGREGATION NODE ARCHITECTURES

Figure 9(a) shows a generic architecture of an optical switching node envisioned in the PASSION project. At the heart of the PASSION node is the photonic switch providing connectivity between the express and add/drop traffic. It consists of optical switching components for handling express traffic, added traffic and dropped traffic. The S-BVTs attached to the switching node are used to transmit the locally generated traffic with flexible allocation of bandwidth and hence data. The capability of the S-BVT to generate traffic with variable bandwidth based on the bandwidth granularity is used to fulfill the agile capacity requirement of the nodes. The locally generated traffic and aggregated traffic are merged as added traffic. The switching functionality is implemented via photonic switches, add switches, aggregate/disaggregate switches, and multicast switches (MCS). These last derive the dropped traffic to the coherent receiver modules (CRMs). Photonic switch provides space-based switching of the traffic at any input port to any output port which are either assigned to express out path or dropped traffic path. The architecture incorporates modularity as highlighted in the shaded blocks of Figure 9, where new modules are incorporated to meet the capacity requirements in a pay-as-you-grow fashion.

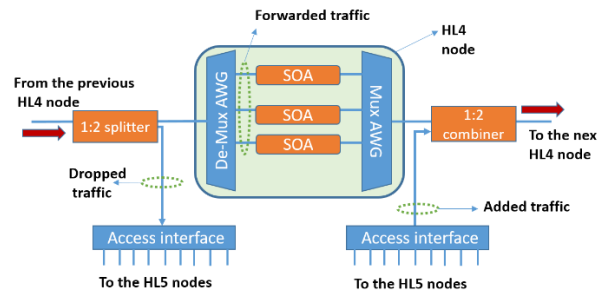


(a)





(b)



(c)

Figure 9 (a) modular design of PASSION switching node within metro-core network (b) modular design of PASSION switching node (HL 1/2 and HL3) within metro-core network adapted to the use cases (c) schematic representation of the envisioned HL4 nodes

The Aggregate/disaggregate switches do the routing of the dropped traffic either to the MCS switch or Add switch on the level of wavelength granularity. The Add switch provides merging and aggregating tasks for the wavelength division multiplexing (WDM) inputs originating from S-BVTs or directly from the Aggregate/disaggregate switch to the add ports of the photonic switch. The aggregate/disaggregate switch functionality minimizes the complexity of the subsequent nodes in the network by bundling traffic belonging to the same destination together. In this way, the available transmission resources are efficiently used. The drop part diverts some of the link traffic to drop it at the receiver side. For this purpose, the MCS enables colorless and contention-less switching to efficiently use the available coherent receiver modules (CRMs).

3.1 HL1/2, HL3 NODES

Figure 9(b) shows the architecture of an optical switching node envisioned in the PASSION project adapted to the use cases of HL1/2 and HL3 nodes. The HL1/2 and HL3 nodes have the same architecture and functionality, on the other hand, the HL1/2 can accommodate larger network traffic compared to HL3 nodes. This is because, the HL1/2 nodes are used to aggregate traffic from several HL3 and HL4 nodes as explained in Section 2. The main difference between Figure 9(a) and Figure 9(b) is that, the add and drop signal paths are connected to the HL4 node instead of the S-BVT and CRM respectively. This is because in the presented use-case #3 no local traffic is aggregated directly at HL3 node. The generated traffic from HL4 nodes is added to the Add switch of either HL1/2 node or HL3 node depending on the specific path. The locally generated traffic and aggregated traffic are merged as added traffic. On the drop side the traffic destined for the HL4 nodes is disaggregated towards the HL4 ring network.

3.2 HL4 NODES

The HL4 nodes are implemented with low cost switches based on wavelength blockers for a simple add/drop functionality. The schematic representation of the envisioned HL4 nodes is shown in Figure 9(c). It typically consists of a de-multiplexing Arrayed waveguide grating (AWG) at the input. The HL4 nodes are connected via a WDM link in a ring topology. At each HL4 node a 1:2 splitter is used to tap the drop signal, which is broadcasted to a number of splitters to HL5 nodes. A tunable filter at the input of the HL5 nodes enables a colorless and directionless drop of signals. The wavelengths destined to the local HL5 nodes will be blocked by the semiconductor optical amplifier (SOA) gate switches. On the other hand, wavelengths destined for the next HL4 node are passed by the turning on the SOA gate switches. On the add/drop side, an access interface is used to handle traffic from /to all HL5 nodes. This low-cost implementation of HL4 nodes targets the use of commercial deMux/Mux Arrayed waveguide grating and SOA gates at channel spacing of 50 GHz.

3.3 ADVANCES IN PASSION NODE ELEMENTS

In this section, technological advancements and progresses in the switching elements are reported.

3.3.1 Photonic switch

Partner institution ETRI has reported the implementation of 16x16 photonic switch based on polymer matrix has been finalized. As shown in Figure 10 below, the switch is fully integrated with control circuit board.

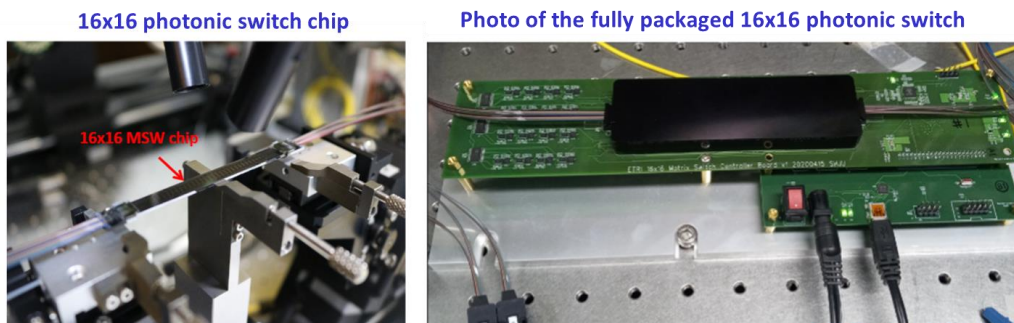


Figure 10 Implementation of 16x16 polymer matrix photonic switch

3.3.2 Add/drop wavelength selective switch (WSS)

Tu/e in collaboration with partner institution VTT has developed a hybrid wavelength blocker (WBL) which is the fundamental building block in wavelength selective switches that can be used in the add/drop path of the switching node. The design is based on *broadcast-and-select* scheme, in which the signal is broadcast by a $1 \times m$ splitter and is selected by m wavelength blockers (WBLs) at the output ports. The purpose of hybrid integration is to exploit the loss-less SiPh platform together with InP SOA switch to enable no-loss or very low-loss switching performance.

The current implementation consisted of two WBLs centred at 1546.52 nm and 1546.72 nm. The number of channels n of the WBLs is 10, therefore 16 of these modules will be used to cover the whole C-band of 160 wavelengths. The channel spacing of the WBL is 100 GHz.

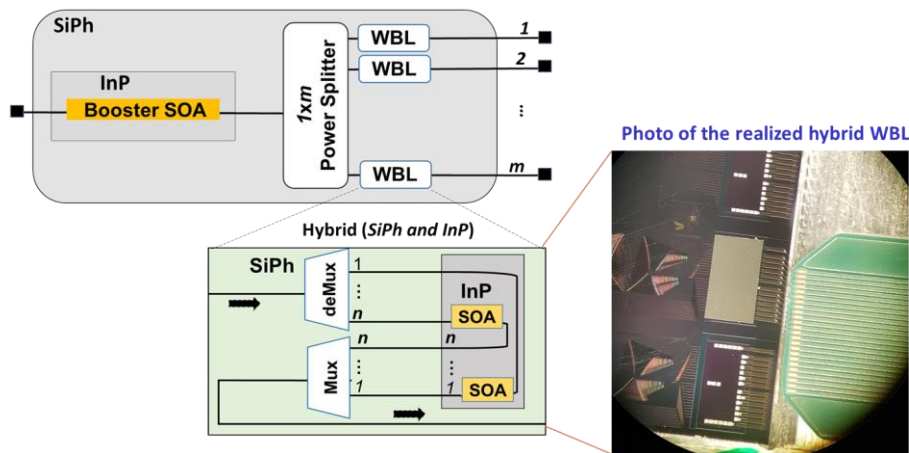


Figure 11 Implementation of hybrid WBL for WSS in the add/drop path

The WBL is constituted by de-multiplexing/multiplexing circuitry on SiPh and InP SOA switching gates as illustrated in Figure 11. The hybrid WBL is based on SiPh deMux/Mux circuits and SOA switching gates on InP chip. The integration scheme used cavities on SiPh chip to flip-chip bond the InP chips after fabrication. Currently, this circuitry is used under test.

3.3.3 Multicast switch (MCS)

One of the switching functionalities in the node is multi-cast switching as previously explained. Accordingly, hybrid multi-cast switching functionality is implemented via passive SiPh circuitry together with and InP SOA arrays that serve as both gate switches as illustrated in Figure 12. The circuit implemented 1x2 MCS functionality while also emulating large scale integration (8x8 MCS) by accommodating extra input/output ports (labeled in Figure 12 as *broadcasted input* and *broadcasted output*). Therefore the 9 SOAs within InP are used: 1 SOA is used for boosting (amplification) and 8 SOAs are used as gate switches.

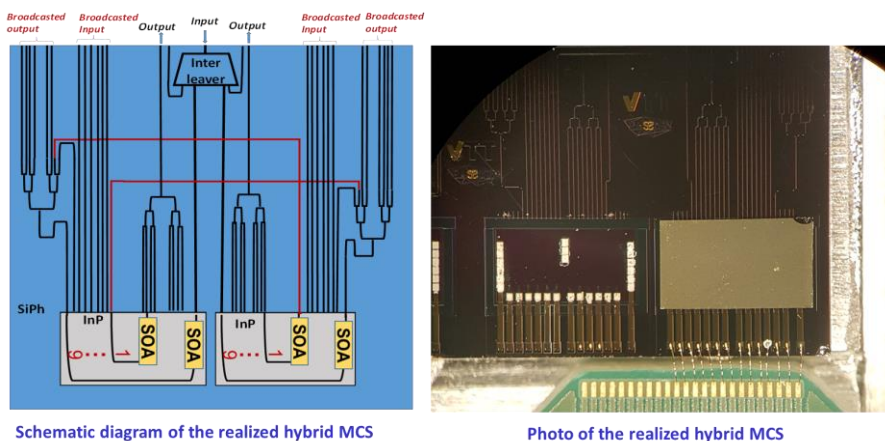


Figure 12 Schematic and photo of the realized hybrid MCS

The flip chip bonding of InP SOA arrays into SiPh circuitry was done by partner institution VTT.

3.4 CONTROL ASPECTS OF SWITCHING NODE

The control of the switching node is handled by the central SDN controller. The control of the switching node involves the following physical parameters of the switch:

- The central frequency of the channel for the WSS units in the add/drop path



- Input port of the switch
- Output port of the switch

The dynamic control of the above parameters will be used to meet the traffic requirements of the network while avoiding contention.

In particular, as detailed in D2.2, three types of ports (portType) are defined i) Add: these ports are attached to the S-BVT Tx to enter the optical signal towards the network; ii) Drop: these ports are connected to the S-BVT Rx to receive optical signal arriving from the network; iii) Express: these ports provide the physical connectivity to other optical switches. In general, both directions are supported for the express interfaces. For each port it is needed to provide information related to the supported nominal central frequency and slot width granularities. As specified in D2.2, this information is considered by the SDN controller to determine the optical flow occupation or frequency slot, in terms of central frequency (n) and slot width (m) [ITU].

4 PASSION TRANSCEIVER ARCHITECTURE

In this section, the PASSION transceiver architecture is detailed focusing on the different elements composing the transceiver, including the transmitter and the CRM supporting the high capacity connections over extended distances. Particular attention will be devoted to the modularity and related implementation choices according to the adopted photonic technology solutions. For the modular transceiver design, the considered schemes for the transmitter and receiver architecture are described taking into account an optimal usage of the available resources and dimensions, including optical spectrum, modulation format and SDM (fibre bundles or MCFs), to address the target capacities and use cases.

4.1 S-BVT ARCHITECTURE

The S-BVT modular architecture, programmable via the SDN platform described in D2.2 [D2.2], is presented in Figure 13 as part of the PASSION system architecture, including the node architectures for the different HL, as detailed in Sec. 3. This allows to better specify the adopted solutions and their interrelationship.

The S-BVT Tx and Rx are separately indicated with the corresponding agents, attached to the specific node type, to emphasize the considered modular options and features according to the use cases of interest. As mentioned in Sec. 2.2, simpler cost-effective transceiver and switching technologies are envisioned for the lower level HL4 nodes, handling only the spectral dimension, while fully featured S-BVT, equipped with multiple modules, are adopted for upper HL nodes enabling the management of both the spectral and spatial dimensions. In the IP offloading use case (# 3, described in Sec. 2.1), HL3 nodes are transit nodes.

The S-BVT Tx modules are based on large bandwidth VCSEL sources enabling the generation of multiple flows, activating/de-activating the appropriate source(s). As shown in the bottom left-hand inset of Figure 13, the SOI chip fundamental building block integrates 4 submodules, each equipped with 10 VCSELs, at operating wavelengths covering the C-band. At the Rx side of the S-BVT multiple modules (CRMs) based on integrated CO-Rx are adopted. The fully equipped S-BVT Tx is also depicted in the bottom right inset of Figure 13, for the sake of clarity, completing the architecture description of the S-BVT attached to higher HL nodes (HL2/1). As cost-effective alternative for the Rx module, direct detection (DD) could be also envisioned. However, in order to support the targeted metro network paths and most demanding use cases (e.g. #1 and #3), CO-Rx is the most preferred



choice ensuring to achieve ultimate performance, as demonstrated in [Sva20] and reported in this document in Section 5.2.3.

Sub-wavelength granularity and variable bandwidth adaptation (per flow) are enabled by the adaptive digital signal processing (DSP) block using MCM, either discrete multitone (DMT) or orthogonal frequency division multiplexing (OFDM). Bit loading and power loading (BL/PL) optimal or sub-optimal algorithms, such as the Levin-Campello or Chow’s algorithm, are applied to take into account the signal-to-noise ratio (SNR) per subcarrier [Sva16] and the target rate or performance (margin adaptive, MA, or rate adaptive, RA, options/modes). Therefore, the flow is adapted to the required bandwidth, traffic demand and quality of transmission required by the established connection. The DSP in addition to the adaptive MCM blocks, in case of CO-Rx also include specific blocks for the correct recovery of the in-phase and quadrature components [Fab20A]. However, it should be mentioned that, since intensity modulation is performed with the direct modulation (DM) of the VCSELs, the proposed architecture requires a simplified CO-Rx post-processing, enabling chromatic dispersion (CD) compensation and the retrieving of the original intensity signal by applying the square modulus function [Sva19A, Bof20, Fab20A].

As it will be analyzed in Section 5, it is assumed that up to 50 Gb/s capacity is supported per flow adopting this approach with CO detection, thus a submodule would provide up to 500 Gb/s. The fundamental module (SOI chip), aggregating 40 flows (if all the VCSELs are enabled by the SDN controller), can provide up to 2 Tb/s capacity. Thus, with a super-module including 4 fundamental modules, the C-band is covered with 160 (25GHz-spaced) channels at 50 Gb/s, yielding a total capacity of 8 Tb/s. By considering the polarization dimension, the capacity is doubled to 16 Tb/s and including the spatial dimension (e.g. 7-core fiber or a bundle of 7 fibers) more than 100 Tb/s can be supported.

In the next sections, further details on the modular Tx and Rx architectures are provided.

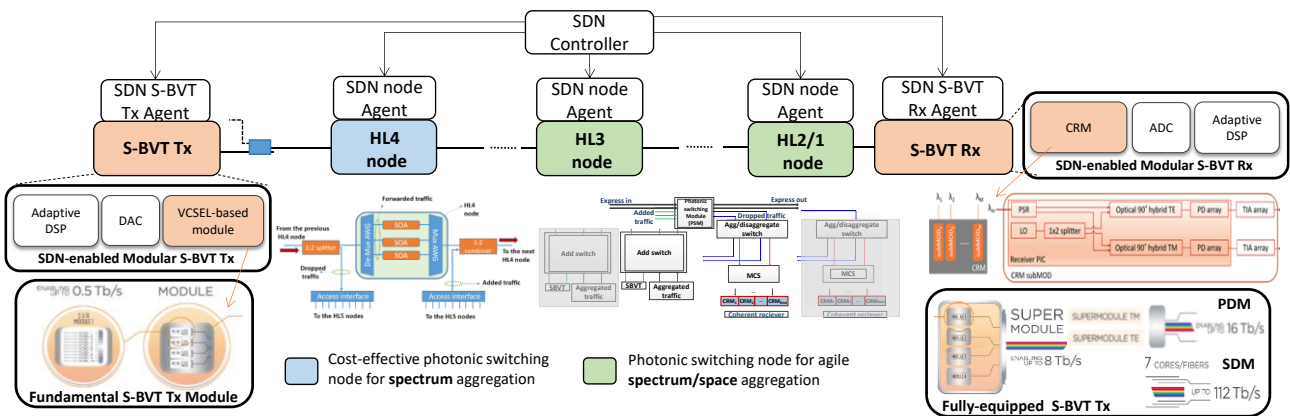


Figure 13 PASSION photonic system including S-BVT modular architecture and subsystems; insets detailing the Tx and Rx modules. Also, node architectures are included.

4.1.1 PASSION Transmitter architecture

As previously introduced, the PASSION Tx architecture adopts a modular approach based on the use of long-wavelength VCSELs, as described and specified in MS6 [MS6], that we report here with recent advances on the technology solutions developed within WP3 [Bof20, Bha19].

The basic, fundamental element on which the S-BVT Tx is based on is the VCSEL. It is in InP, photonic integration platform enabling to operate within the C-band by exploiting the buried tunnel



junction (BTJ) approach. Single-mode operation is achieved by an appropriate transverse waveguide structure with sidemode suppression ratio higher than 35 dB and a stable polarization output. The reduced active area allows an expected far field confinement of less than 12° with a structure optimized for massive integration. In order to achieve large modulation bandwidths, it is beneficial to reduce the effective cavity length and the photon lifetime in the VCSEL cavity [Wes11]. Therefore, the high modulation bandwidth (beyond 18 GHz) targeted for the PASSION Tx architecture, enabling to achieve up to 50Gb/s signal rate per each VCSEL flow, requires a short-cavity (SC) design. This is achieved by means of a very short resonator length and an active region optimized for high bandwidth, as shown in Figure 14. The long-wavelength SC-VCSELs produced by VERTILAS to be integrated within the PASSION Tx modules target very low power consumptions (< 35mW) with output power about 4 mW at 20°C and low threshold current (< 2.5 mA at 20°C) [D3.2]. BTJ active area is maintained small (<5.5 μm) to optimize the SOI waveguide coupling in the PASSION Tx design.

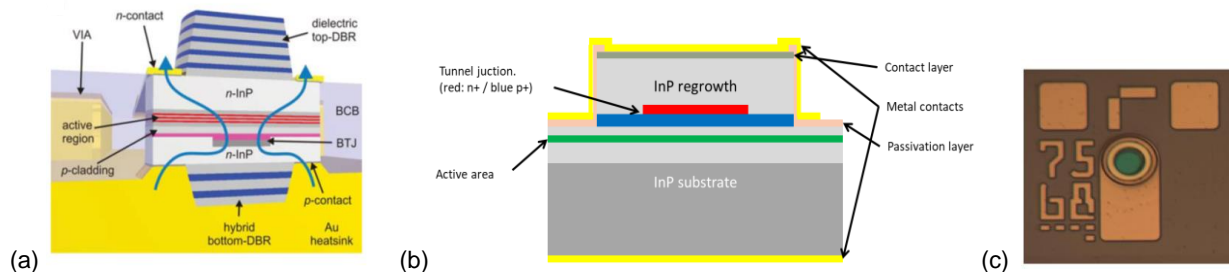


Figure 14 SC-VCSEL (a) optimized structure for high modulation bandwidth; (b) BTJ structure; (c) device picture.

The PASSION VCSELs are designed to target different emission wavelengths covering the C-band. Taking into account the ITU-T WDM channel grid, for the Tx architecture design the considered frequency range is from 191.900 THz (corresponding to the CH19 or wavelength 1562.23nm) to 195.900 (CH59 or 1530.33nm), being 195.875 THz (CH58) the last nominal central frequency as operating VCSEL wavelength. As previously introduced, the VCSEL (or optical flow) nominal central frequency can be also indicated in terms of n , according to [ITU] for flexi-grid. This allows implementing the fundamental module (MOD) of PASSION Tx architecture, as depicted in Figure 15. There, it is also shown the corresponding VCSEL operating wavelengths per each one of the four submodules (subMOD) belonging to the specific fundamental module (the first one, indicated to as MOD-1). Additionally, each VCSEL could be finely tuned within a 25GHz channel grid through current tuning.

As each VCSEL is assumed to be directly modulated adopting MCM to provide up to 50 Gb/s (capacity per flow with 100 GHz spacing), the PASSION fundamental module provides up to 2Tb/s transmission capacity. This element is the one considered to be attached to HL4 nodes and the building block for composing the fully equipped S-BVT Tx (see Figure 13).

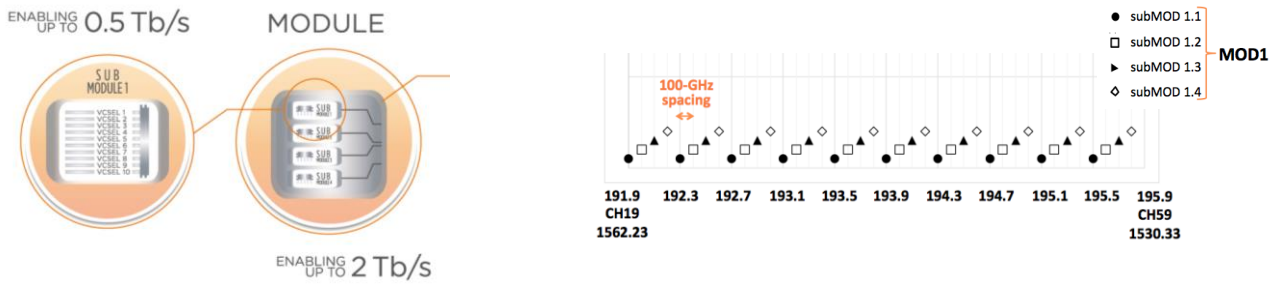


Figure 15 SOI on chip module and wavelength assignment, expressed in THz, nm and corresponding ITU-T channel, per submodule element (MOD-1).

The fundamental module is integrated into a Silicon-On-Insulator Photonics Integrated Chip (Si-PIC), as shown in Figure 16. All necessary building blocks combined on a single Si-PIC chip to form a full module (MOD1) architecture and the related mask designs, together with innovative integrated mirror designs have been successfully carried out.

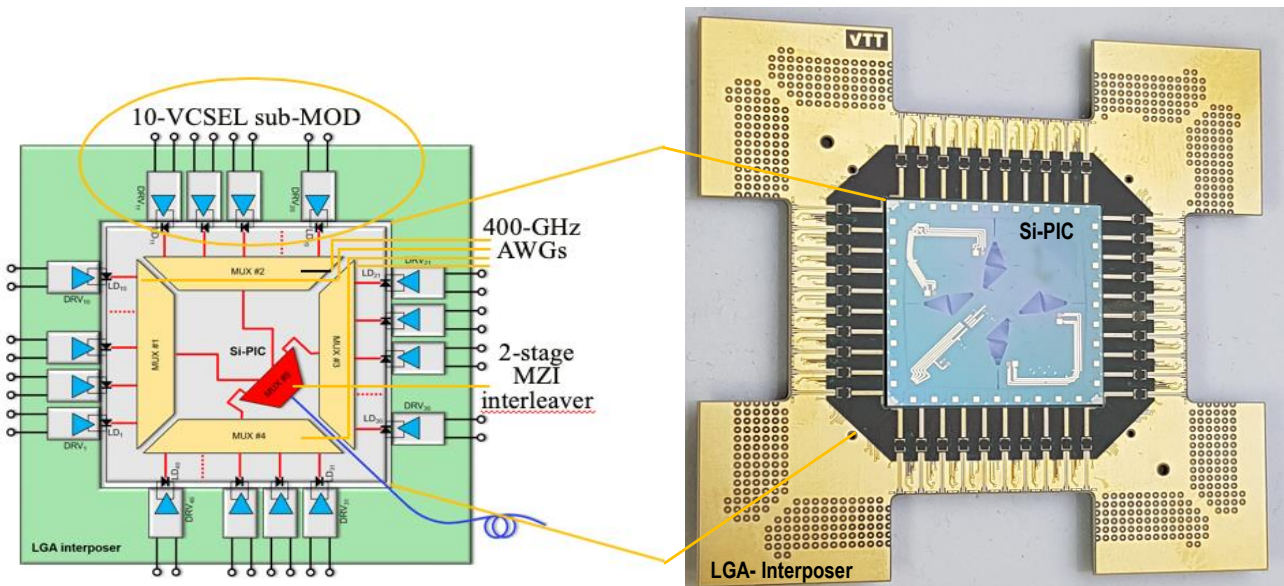


Figure 16 The 2-Tb/s fundamental module architecture and LGA interposer design to interconnect Si-PIC to driver electronics.

The design for the fundamental module architecture that combines 40 channels (ITU 19-58) with a spacing of 100 GHz is shown in Figure 17 (left). This is being fabricated as part of the VTT MPW 6 process run. The mask design fabricated chip is shown in Figure 17 (right).

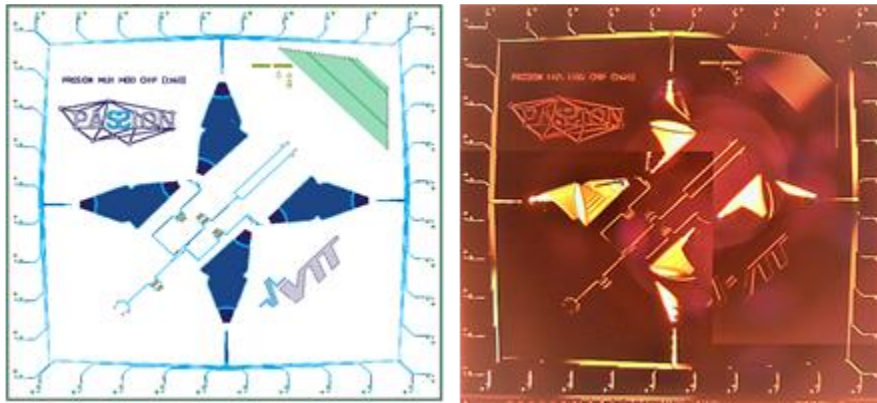


Figure 17 MOD1 design – Mask design (left) and image of the fabricated (partial) chip (right)

The complete optical design for the full MOD1 architecture can be broadly classified into three separate design elements as listed below, which are discussed in more detail in further sections:

- Up/down-reflecting 45° TIR mirror design to coupling VCSEL power into SiPh waveguides as well as to couple light output from the Si-PIC chip into a (PM) fiber.
- Ten inputs-one output, 400 GHz channel spacing AWG multiplexer designs for the four sub-MODs
- Interleavers design (with two stages MZI) to multiplex the four sub-MODs outputs into a single output waveguide.

Integrated optical mirrors on Si-PIC in both *up-reflecting* and *down-reflecting* configurations (accordingly to top-mounted VCSELs or bottom-mounted VCSELs respectively) are currently under investigation. In the MOD1 design, up-reflecting mirrors are considered a good solution to efficiently address optical beams from VCSELs into waveguides as well as to deliver optical signals toward a fiber optic assembly (Figure 18). Preliminary measurement results (report D.3.3) indicate a good agreement with the design targets (test performed by VTT). Mirror coupling-losses of less than 0.5 dB when interfacing with a polarization-maintaining fiber (PMF) have been obtained over the entire C-band in both TE/TM polarizations.

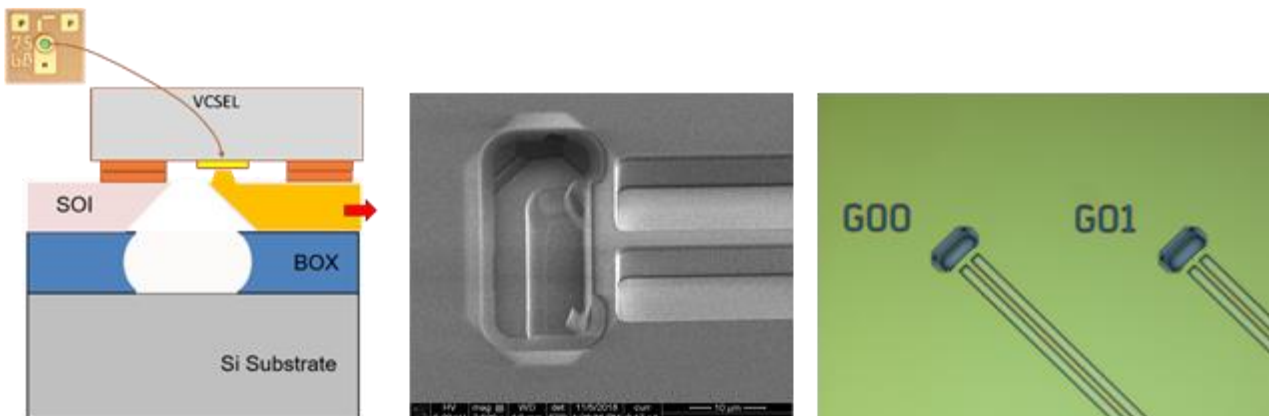


Figure 18 Schematic for VCSEL solder bonding on Si-PIC up-reflecting 45° TIR mirror design (cross section view, left), fabricated up-reflecting mirror for VCSEL optical coupling (middle and right).

Each ten-channel sub-MOD MUX with channel spacing of 400 GHz has many advantages (from a design perspective) both in terms of flexibility and fabrication tolerances. An individual S-type AWG

design (see Figure 19) has been implemented for each of the sub-MOD with the free spectral range (FSR, 8 THz) centered at ITU channel wavelengths 37, 38, 39, and 40, which also corresponds to the center of each of the four sub-mod channel bandwidths.



Figure 19 Schematic design (left) and mask design (right) of an S-type 10 channel AWG sub-MOD MUX design with a channel spacing of 400 GHz.

To electrically interconnect the SI-PIC with the VCSEL sources, an *electrical interposer* based on a Land Grid Array (LGA) pads architecture has been designed to route 648 DC lines (including ground distribution, DC power supplies and digital controls) as well as 160 critical RF lines (25 GHz) for a total amount of 808 pads (Figure 20).

Furthermore, to initially test and characterize MOD1 (Si-PIC assembled on LGA interposer), a specific evaluation board will be designed and exploited as test vehicle before the final implementation of the MOD1 on the main PCBs of S-BVT architectures.

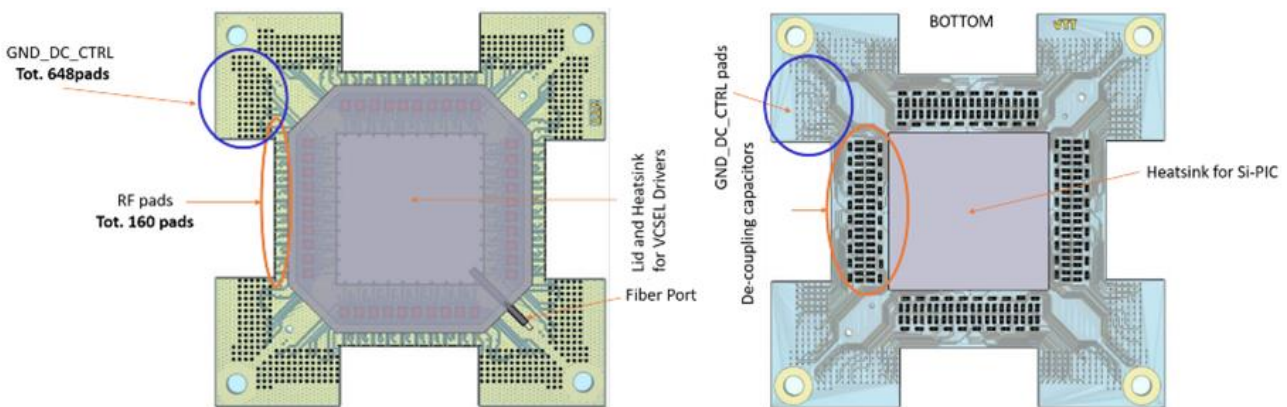


Figure 20 Land Grid Array pads architecture.

The PASSION super-module is modularly composed by combining four PASSION fundamental modules based on the approach above described (namely MOD1, MOD2, MOD3 and MOD4), as shown in Figure 21. Each fundamental module is equipped with the 40 VCSELs enabling multiple 100 GHz spaced flows, at operating wavelengths shifted of 25 GHz with respect to the ones of the VCSELs in the adjacent modules (see Figure 21, wavelength assignment). Thus, if each VCSEL flow enable to support up to 50 Gb/s (capacity per channel with 25 GHz spacing), the super-module is able to provide up to 8 Tb/s capacity by fully exploiting the spectral resource, within the C-band range from CH19 to CH58 (191.900 THz – 195.875 THz). The multiple flows at the output of each module are suitably aggregated (single sided) by means of a WSS.

The modular approach also allows to compose the S-BVT Tx, according to the node type and network need/upgrade. For example, also 50GHz-spaced channels/flows can be obtained by suitably combining only two modules (e.g. MOD-1 and MOD-3 or MOD2 and MOD-4), obtaining a maximum supported capacity of 4 Tb/s.

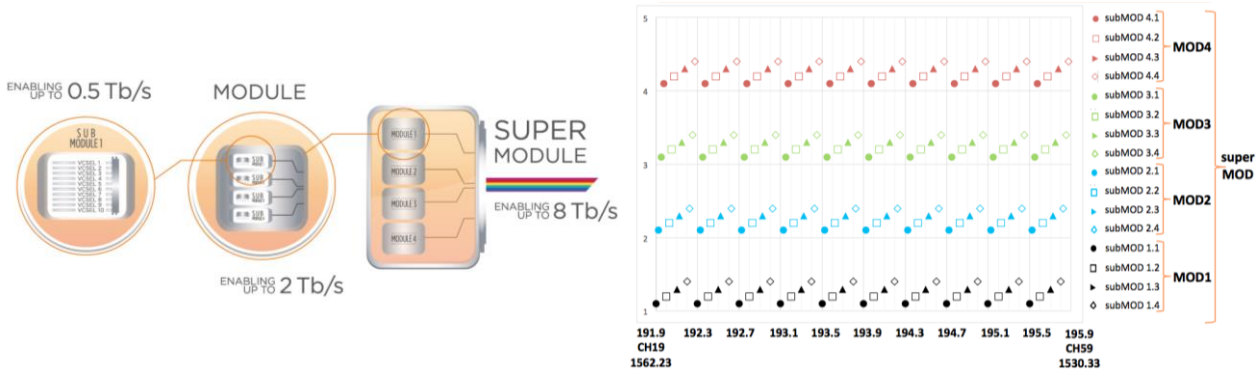


Figure 21 Module with sub- and super-module and corresponding VCSEL operating wavelength in THz, nm and ITU-T channel, per Tx element.

The architecture further scales to higher capacity with additional (> 4) modules, considering the polarization dimension and/or the spatial dimension, as shown in Figure 22. Particularly, the polarization division multiplexing (PDM) allows doubling the capacity up to 16 Tb/s. The envisioned Tx architecture requires two PASSION super-modules for a total of 8 modules: the transverse electric (TE) and transverse magnetic (TM) super-modules are multiplexed with a polarization beam combiner, as shown in Figure 22. With space division multiplexing (SDM) the capacity can be enhanced by a factor depending on the number of adopted/available fibers/cores. Thus, a total capacity above 100 Tb/s is achieved with PDM and 7 fibers/cores.

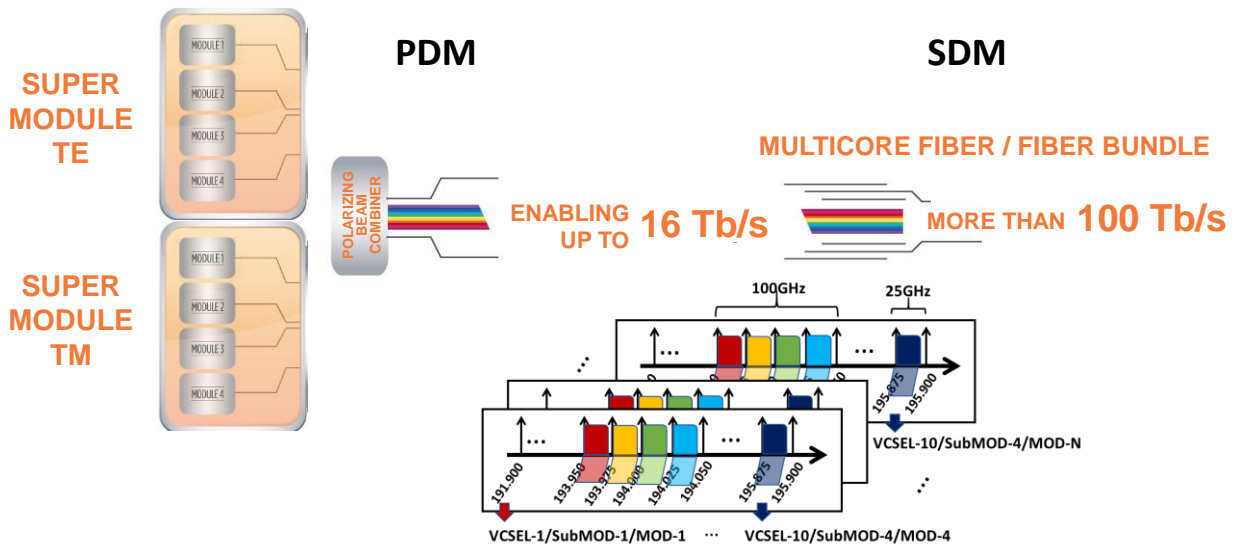


Figure 22 Super-module PDM and SDM with corresponding achievable capacity and Tx element/dimension assignment.

4.1.2 PASSION Receiver architecture

At the receiver (Rx) side, the S-BVT architecture is based on a set of integrated CO-Rx submodules. The complete multichannel CRM consist of M dual-polarization submodules, as shown in Figure 23. Each submodule contains a tunable local oscillator (LO). The LO in each submodule can be

individually tuned to a suitable central channel frequency to recover the transmitted flows. As mentioned in PASSION deliverable 4.6 [D4.6], the submodule approach was chosen for yield and therefore cost reasons.

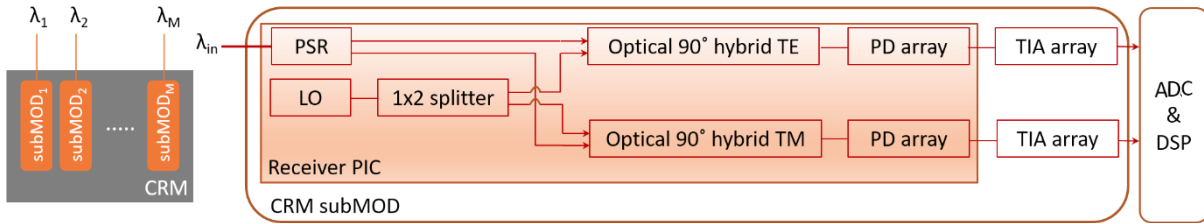


Figure 23: Multichannel CO-Rx module (CMR) and submodule schematic

A three-staged approach was chosen to develop the CRM. Stage 1 focusses on the development of the individual building blocks necessary to deliver the required functionality. In stage 2 these building blocks are monolithically integrated on a single chip. The third and final stage incorporates this chip into a test-bed for evaluation by the rest of the consortium. This is illustrated schematically in Figure 24. Stage 1 was reported on in [D4.2], stage 2 was reported in in [D4.6]. Phase 3 is currently being worked on.

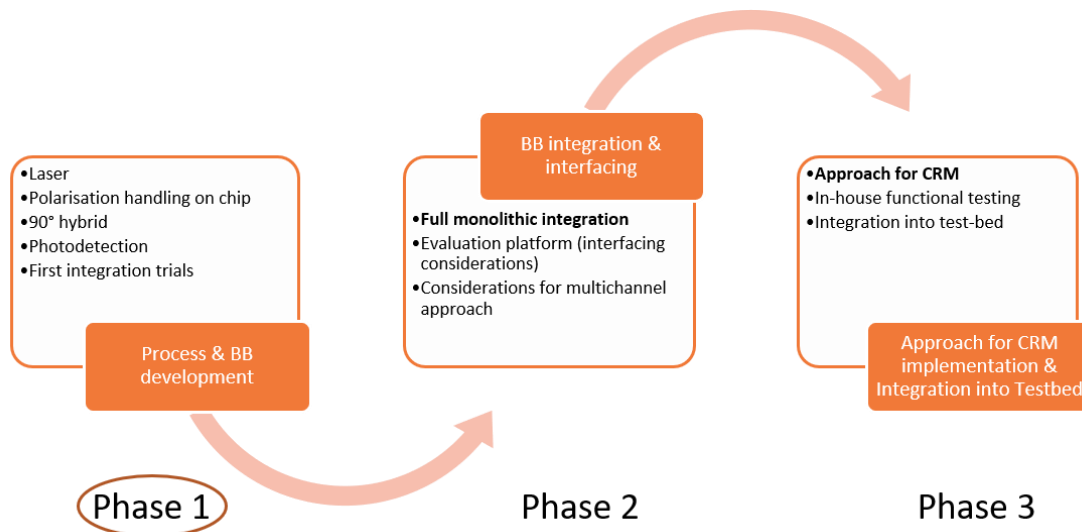


Figure 24: Staged CRM development approach

4.1.2.1 Module design

A CRM concept with two submodules is shown in Figure 25. Each submodule is built around an optical subassembly (OSA) that includes a fully integrated polarization multiplexed coherent receiver (PIC) directly connected via wire bonds to a quad-channel 64-GBd capable Transimpedance Amplifier (TIA). Both the PIC and the TIA are wire-bonded and die-bonded to an Aluminium Nitride (AlN) multilayer tile. The multilayer AlN tile serves as electrical interconnect for the DC bias signals to both the PIC and TIA and it also provides the proper heat-spreading required for the thermal management of the complete OSA.

The multilayer (4-layers) AlN tile connects, up to 56, active signals which are fanned-out to two of its edges. To prevent electrical noise coupling, an array (6x) of bypass capacitors 100pF/each is die-bonded to the tile ground plane as close as possible to the TIA. The OSA thermal monitoring uses

an NTC (negative temperature coefficient) directly die-bonded next to the PIC. The optical signals from/to the PIC are coupled to a polarisation maintaining fibre array (4x) mounted on AlN spacer tile for each of the CRM submodules.

The multilayer tile is then wire-bonded to a high-speed PCBA to breakout all the connections to both a 56pin DC ribbon connector and an RF GPPO connector array (8x). The 3-layer PCBA has been engineered to operate at up to 40GHz of 3dB analogue bandwidth with a stack up engineered with Rogers material (RO4350B) for the coupled coplanar waveguide (CPWG) 100-Ohm differential traces from the TIA to the RF connector array.

The two CRM-submodules, each with dimensions of 6cm x 3cm x 1cm (W x L x H) are mounted on top of an aluminium heat spreader which sits on the cold side of a shared thermoelectric cooler (TEC) with its hot-side attached to a heat-sink. The overall CRM dimensions are 7cm x 7cm x 2cm (W x L x H). As shown, the CRM architecture addresses the need for modularity and ease of expansion for throughput capacity scaling.

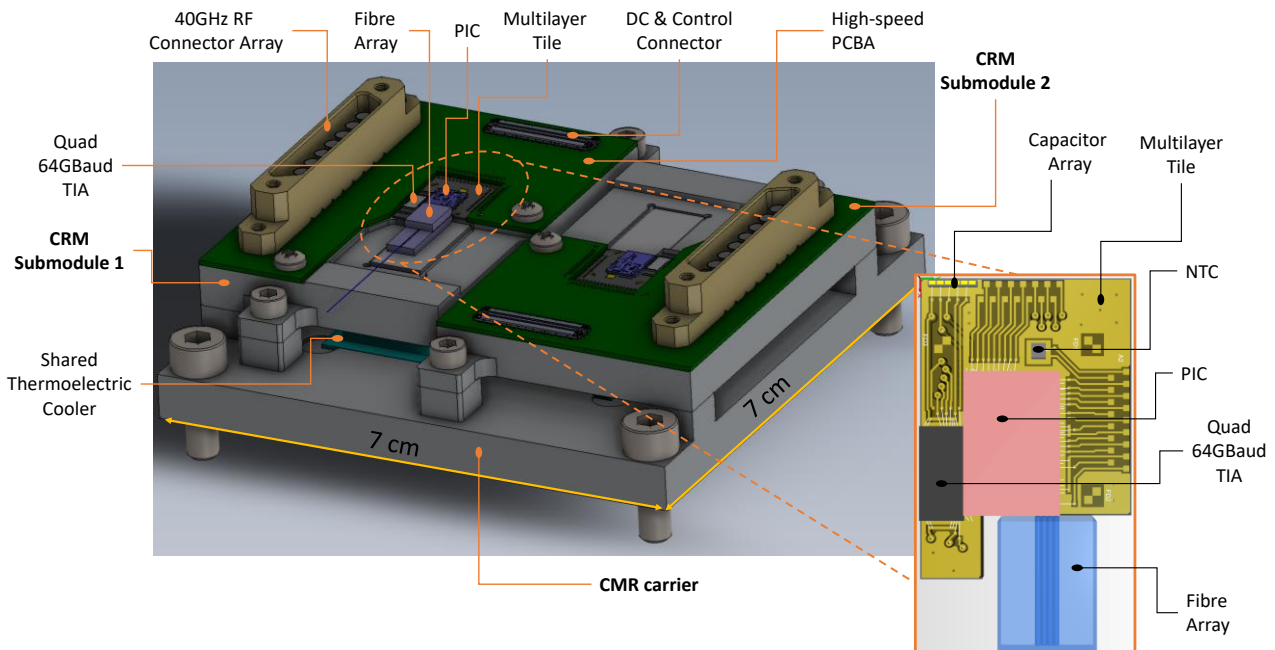


Figure 25: Overview of the CRM submodule assembly

4.1.2.2 Chip design

A fully integrated CRM chip design was made in HHI's MPW platform [HHI]. This technology allows to integrate lasers, passive splitters, polarization handling and spot-size converters in a single chip. Figure 26 shows the design of the chip and highlights some of the major parts. On the righthand side an array of four spot size converters (SSCs) take a 10 μm SMF fiber mode and transform it down to a 2 μm waveguide mode. The SSCs are 250 μm apart, which facilitates coupling to standard fiber arrays. The top fiber is used to calibrate the on-chip LO. Alternatively, this fiber can also be used to launch an off-chip LO as a fallback option incase the on-chip LO does not function. The third fiber from the top is the main input, which accepts a polarization multiplexed signal. For mitigation in the design stage, a X bypass and Y bypass is included. These can be used when the polarization splitter

and rotator on the chip are not meeting specifications. To be able to use these bypasses an external polarization rotating beam splitter is needed, combined with a polarization maintaining fiber array.

After the polarization handling stage, the bypass is recombined with the main path and feeds into a separate pre-amplifier for the X and Y polarizations. The pre-amplifiers can be used to attenuate or amplify the signal, depending on the current supplied to them. The X and Y signals are then fed into two 90 degree hybrids, that terminate into a total of 8 fast (>40 GHz bandwidth) photodiodes.

The chip has three possible LO sources: an on-chip ring laser, an on-chip DBR laser, and an off-chip laser. From the on-chip sources, the ring laser is expected to have the lowest linewidth and intensity noise. The DBR laser is included as a fallback option in case the ring laser is not meeting specifications. Additionally, the DBR laser provides a study into a possible low-cost LO option. The DBR laser has fewer components, which will result in higher yields. Furthermore, the DBR laser is smaller in size than the ring laser, which leads to a smaller and therefore cheaper chip. At this point it is unknown whether the DBR laser has a high enough performance to meet the requirements of PASSION. Before entering the X and Y hybrids, the LO passes through separate boosters. This allows for balancing of the LO power over the X and Y hybrids.

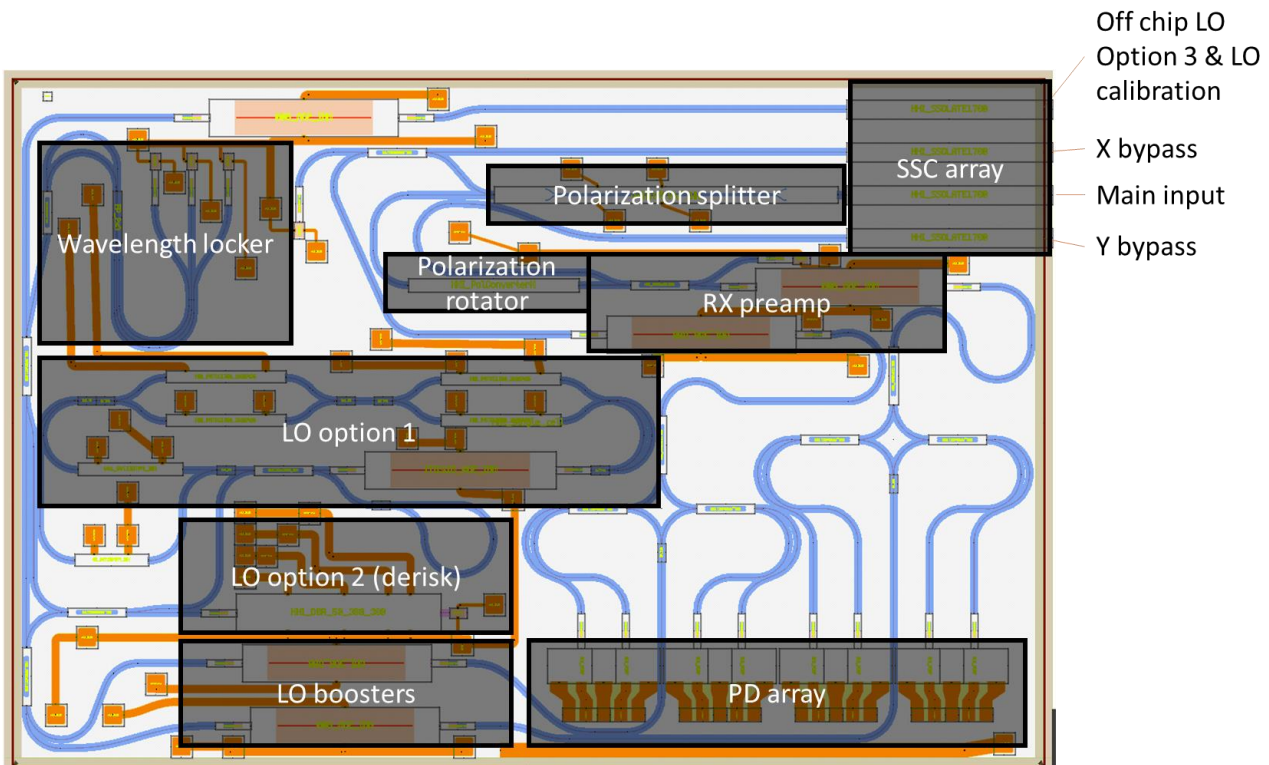


Figure 26: CRM photonic integrated circuit design

4.2 MODULARITY AND PROGRAMMABILITY

Modularity and programmability are key features strictly related to facilitate disaggregation and interoperability, while easing adaptation and flexibility to network upgrade, and ensuring future-proof scalability to the network needs and requirements. The PASSION SDN-enabled S-BVT is designed to be adaptive to multiple rate/reach according to the traffic demand and selected path, for a target performance, offering a wide range of sub- and super-wavelength granularities. Spectral/spatial aggregation and slice-ability are enabled, fully and optimally exploiting all the available resources/dimensions according to the SDN controller decisions [Sva19B].



Due to the limited tune-ability of the optical source(s) at the Tx, the PASSION S-BVT architecture, following the modular approach described in Sec. 4, has been carefully designed to overcome/mitigate this limitation and provide the modules with enough flexibility to be used in future agile MANs. The VCSEL are designed to operate at specific wavelengths, assigned in order to cover the C-band, with flow/channel spacing of 400 GHz per submodule and 100 GHz per each SOI chip module. Adding modules, the spectrum can be fully populated with 25 GHz spaced channel. Each VCSEL can be enabled/disabled to suitably set-up a connection in the MAN at the target capacity, by aggregating multiple flows generated at different modules [Mar19]. Thus, variable granularities are obtained and can be differently managed by the different node types: 100GHz and 50GHz granularity at HL4, while a wider granularity range including 25GHz can be addressed at HL3 and HL2/1 nodes, for finer aggregation and disaggregation of the flows, according to the node architectures and functionalities described in Sec. 3.

Furthermore, the use of MCM allows obtaining a sub-wavelength granularity of the order of tens of MHz at the digital/electrical level, according to the DMT/OFDM subcarrier number. This number can be flexibly adapted at the DSP, according to the target requirement or module design/type. The adaptability and flexibility of the solution is further enhanced by adopting BL/PL algorithm at the DSP. Optimal or suboptimal bit number and/or power per subcarrier are assigned according to the channel state information (CSI) retrieved at the Rx by transmitting a probing (uniform loaded, UL) signal (generally 4QAM format is used over all the subcarriers). An example of bit assignment with corresponding CSI is shown in Figure 27(a), for 512 subcarriers of an OFDM signal with optical spectral occupancy of 12.5 GHz to be transmitted over a single-hop path of 35 km SSMF [Sva19A]. According to this approach, the rate can be maximized at a fixed performance activating the rate adaptive (RA) mode option of the BL/PL assignment, and the performance can be maximized at a fixed rate with margin adaptive (MA) BL/PL algorithm, as summarized in Figure 27 (a). Thus, the capacity/performance is suitably adapted to the network traffic demand or specific use case requirements over the established network path.

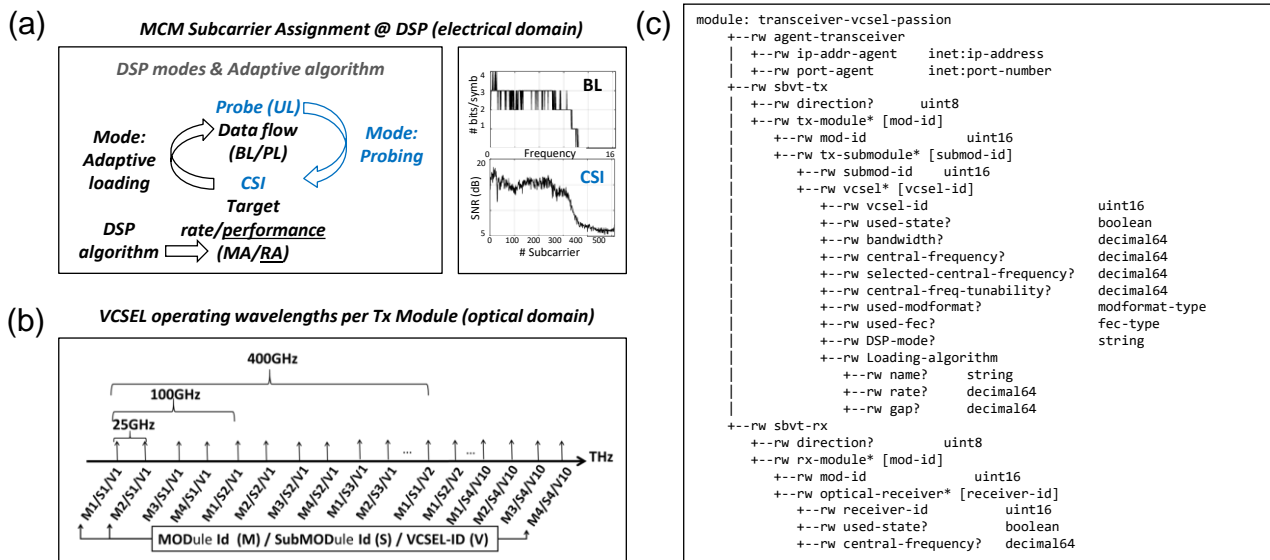


Figure 27 (a) Electrical subcarrier (with example of BL assignment and corresponding CSI) and (b) optical carrier assignment at the S-BVT Tx, tuple and channel spacing identifying the Tx element are indicated. (c) S-BVT YANG model.

In order to suitably enable the targeted S-BVT flow/bandwidth/capacity, each VCSEL should be carefully configured by the SDN controller to operate at the correct wavelength. To do this, the tuple formed by module-id/submodule-id/VCSEL-id (MOD-id/SubMOD-id/VCSEL-id or M/S/V with





corresponding id number) allows identifying a particular VCSEL within the S-BVT, as shown in Figure 27 (b). Similarly, the adaptive DSP parameters and the available resources (in the electrical and optical domain as well in terms of subsystem element and dimension options) should be suitably selected and managed. Particularly, in view of integrating the transceiver within an SDN-based control plane, the model for the SDN-enabled SBVT architecture has been performed, identifying the parameters susceptible to be programmed, according to the designed architecture and the adopted technologies [MS4, Mar19, Sva18].

The information model of any generic system identifies in an abstracted way that relevant information to be taken into account by a controller to achieve the actual configuration of the underlying device, network element, etc. This fosters the definition of the control interactions (i.e., interfaces and protocols) between the centralized SDN controller and the elements (i.e., agents), which directly handle the device configuration.

As anticipated in MS6, yet another next generation (YANG) common data modeling language is used, since it provides a standard way to describe the network/system elements to be controlled and managed. The preliminary S-BVT YANG model presented in [Mar19] has been improved considering also the adaptive DSP parameters/features [Sva18], as shown in Figure 27(c). It is worth notice that, although a set of subsystem attributes are interesting to be exposed to the SDN controller for enabling functionalities/features and correctly setting-up connections, low-level and internal aspects (e.g., circuitry and specific attributes) are hidden and should not be exposed to the SDN controller for an agile management.

The peculiarities of the adopted technologies, such as the limited tunability/flexibility of the laser sources, the combination of direct modulation with CO-Rx and the effect of chirp [Rap18], as further analyzed in Section 5, have been carefully taken into account in the transceiver design and for the S-BVT modeling. This, in fact, is strictly related to the network element programmability handled by the SDN controller. Indeed, the SDN controller configures the transceiver according to a specific set of programmable parameters, being aware of the features, potentialities and limitations of the actual architecture, while computing and setting up an incoming multi-terabit connection request [Mar20].

In addition to the identification of the source element, as above specified, other S-BVT Tx parameters taken into account so far by the SDN controller, as specified in D2.2 [D2.2] are

- *usedState*: to determine if the VCSEL is occupied or unused
- *bandwidth*: for specifying the optical spectrum occupied by each VCSEL. In PASSION, this is set to 20 GHz
- *central-frequency*: determining the central frequency (optical carrier) associated to a given VCSEL within the PASSION spectral range. The central frequency is determined using the ITU-T flexi-grid format, through the *n* value [D2.2, ITU].
- *modulation-format*: specifying the modulation format.
- *fec*: detailing the FEC type

Regarding the S-BVT Rx, the specific CO-Rx is also univocally identified within a CRM with its own identifier, named as *optReceiverId*. The SDN controller refers to the given S-BVT Rx, using both the *nodeId* of the optical switch attached to the receiver device along with the drop port identifier (i.e., *portId*). Other relevant attributes are:

- *usedState*: determining whether a CO-Rx is occupied or available.
- *freqLocalOscillator*: used to specify whether the central frequency of the LO needs to be tuned. The central frequency as in the case of the Tx is determined using the ITU-T flexi-grid format, through the *n* value.

5 OPTICAL TRANSMISSION ANALYSIS AND FEASIBILITY STUDY

In order to evaluate the optical impairment tolerance of the proposed PASSION S-BVT architecture, simulations supported by experimental measurements have been performed.

The reported simulative analysis is based on DMT modulated signals, evaluating both dual sideband (DSB) and single sideband (SSB) transmissions; in both conditions, the generated optical spectra have to occupy less than 25 GHz in order to be transmitted through cascaded filters, present in the network nodes, guaranteeing 25-GHz WDM spacing for fine granularity. For this reason, we test in case of DSB transmission a DMT signal with these characteristics: 256 sub-carriers in 10-GHz range (sub-carrier spacing 39.062 MHz); occupied optical bandwidth around 20 GHz; cyclic prefix (CP) of about 2.1% of the symbol length. On the other hand, the SSB transmission is performed by properly detuning a WSS-like filter with respect to the carrier of a DMT signal with these characteristics: 256 sub-carriers in 20 GHz range (sub-carrier spacing 78.125 MHz); CP of about 2.1% of the symbol length. Figure 28(a) shows the spectrum of the SSB signal obtained detuning the WSS [Pulik11] in order to select half of the 20-GHz DMT DSB spectrum, while preserving the optical carrier. Moreover, Figure 28(b) displays the comparison between the theoretical and experimentally measured spectra of the WSS. As already anticipated in Section 4.1, at the receiver side, as DM is exploited, a simplified CO-Rx is used [Xie15, Sva19A, Bof20, Fab20A]: after I and Q components recovery and chromatic dispersion (CD) compensation, the I and Q square moduli are performed and summed up in order to obtain the originally transmitted intensity signal. This approach avoids the use of phase and frequency recovery, reducing the complexity of the receiver DSP and also relaxing the constraints on VCSEL and LO linewidths. Together with CD compensation, the receiver DSP provides digital symbol synchronization, CP removal, sub-carriers phase recovery, demodulation and error count. In the following the transmitted capacity is evaluated performing Chow's BL algorithm with a target BER of $3.8 \cdot 10^{-3}$ (corresponding to 7% overhead hard decision FEC limit) for single-channel, single-polarization transmission.

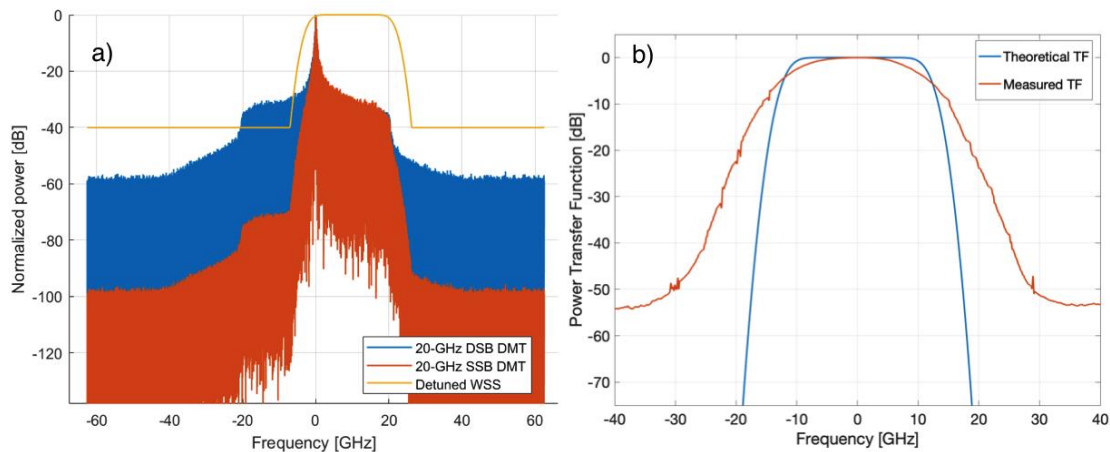


Figure 28 a) DMT SSB optical spectrum (red), obtained by a 9.5-GHz detuned WSS (orange) filtering of a DMT DSB signal with 20-GHz electrical bandwidth and 40 -GHz optical bandwidth (blue). b) Comparison between WSS theoretical (blue) and measured (red) spectra.

5.1 OPTICAL IMPAIRMENT TOLERANCE

The analysis of the optical impairments is performed through the evaluation of the system performance in the case of single polarization transmission; at first, we evaluated the impact of electro/optical (E/O) impairments specifically related to the transmitter (namely chirp and interplay



with node filtering) and to the CO-Rx (LO linewidth, signal-LO detuning, photodiode E/O bandwidth, TIA cut frequency).

Then we analyzed the performance of multichannel propagation according to different network requirements taking into account linear crosstalk due to multichannel propagation and very dense WDM NL propagation, down to 25-GHz channel spacing.

5.1.1 E/O impairments transmitter side

As detailed in MS6, due to VCSEL direct modulation, the PASSION transmitter is affected by the frequency chirp; its interplay with CD can be neglected in case of CO-Rx, where CD DSP compensation can be easily performed, while the impairment due to node optical filtering represents the main limitation. Employing chirp measurements on already-available VERTILAS SC-VCSEL (α linewidth enhancement factor of 3.7 and κ adiabatic constant of $1.52 \cdot 10^{13}$ for SC-VCSELs [Rap18]) the maximum transmitted capacities for both DSB and SSB DMT modulations were evaluated as a function of the number of crossed WSS and of the received OSNR. Further parameters are the VCSEL modulation bandwidth of 18 GHz, which is expected to be achieved in PASSION VCSELs, the 9.5-GHz WSS detuning in case of SSB, the bias current and modulation amplitude of 8 mA and 8.5 mA respectively for DSB and SSB DMT.

Table 5 Transmitted capacities and SSMF reach for SSB DMT as a function of span length and number of crossed WSS.

	OSNR	40 dB	35 dB	30 dB
Reach	35-km span	70 km	210 km	735 km
	65-km span	---	65 km	260 km
SSB	Capacity w 1 WSS	78.6 Gb/s	72.6 Gb/s	57.3 Gb/s
	Capacity w 3 WSS	68.6 Gb/s	63.1 Gb/s	54.5 Gb/s
	Capacity w 5 WSS	61 Gb/s	58.4 Gb/s	50.5 Gb/s
DSB	Capacity w 1 WSS	45.5 Gb/s	30.9 Gb/s	22.8 Gb/s
	Capacity w 3 WSS	35.3 Gb/s	27.5 Gb/s	19.9 Gb/s
	Capacity w 5 WSS	31.1 Gb/s	25.2 Gb/s	19.2 Gb/s

The capacity limits associate with the transmitter E/O response are summarized in Table 5 in case of multi-span transmission with EDFAs with 6-dB NF and SSMF with attenuation of 0.25 dB/km, as a function of OSNR, overall link reach, span length and number of crossed WSS. DSB DMT performance is heavily impaired by chirp and its interplay with filtering, limiting the achievable capacities below 50 Gb/s also for 100-km transmission ranges. Whereas VCSEL-based S-BVT transmitters with SSB DMT modulation can target around 50 Gb/s capacity per polarization also in presence of 5 WSS consecutive filtering for OSNRs above 30 dB. This allows to bridge more than 250 km SSMF for span length of 65 km; with shorter span length, even longer transmission distances could be supported covering indeed wider MANs.

5.1.2 E/O impairments receiver side

As already discussed, with DM the information is encoded in the optical field intensity and thus a simplified CO-Rx can be used; on the other hand, the CO-Rx is not affected by the same impairments



usually faced in case of single-carrier transmission, thus some preliminary evaluations have been carried out. In particular, in case of SSB-DMT, the impact of the LO linewidth was evaluated in combination with a relative detuning of the LO and signal frequencies; the LO power was 10 dBm per state of polarization (SOP), and the photodiodes (PD) had 30 GHz E/O bandwidth and 20 pA/Hz^{1/2}, the 30-GHz PD bandwidth representing the best trade-off for optimizing the received capacity [MS6].

Table 6 SSB DMT capacity in back to back as a function of LO linewidth, LO detuning with respect to the signal center frequency and OSNR.

		LO shift LO linewidth	-5 GHz	0 GHz	+5 GHz
OSNR 40 dB	100 kHz		77.8906 Gb/s	77.0313 Gb/s	76.1719 Gb/s
	500 kHz		77.3438 Gb/s	76.5625 Gb/s	75.7813 Gb/s
	1 MHz		76.7188 Gb/s	76.1719 Gb/s	75.4688 Gb/s
OSNR 30 dB	100 kHz		58.75 Gb/s	58.125 Gb/s	57.4219 Gb/s
	500 kHz		58.3594 Gb/s	57.6781 Gb/s	57.2656 Gb/s
	1 MHz		58.125 Gb/s	57.2656 Gb/s	57.0313 Gb/s

Table 6 results evidences that the impact of the LO linewidth on the PASSION CO-Rx is limited up to 1 MHz and also the detuning of the LO with respect to the SSB spectrum center as a modest impairment (in the 0 GHz condition, a perfect superposition of LO and signal carrier is achieved).

5.1.3 Multi-channel transmission

Before analyzing specific network requirements, we evaluated the cross-talk impact in multi-channel propagation which can be actually ascribed to the transmitter; indeed, in fact, the crosstalk is mainly due to the spectrum broadening induced by the chirp associated with DM [Rap18]. We focused on SSB-DMT, we considered the presence of two adjacent channels to the channel under test and we considered the measured WSS transfer function for both the Tx and the Rx side filters. The analysis evidenced that the presence of the linear crosstalk can reduce the capacity with respect to single channel performance of even 50% in case of a low number of filters. This effect is caused by the presence of a residual component of the adjacent channel located on the higher frequency subcarriers which lowers those subcarriers SNR [MS6]. We demonstrated that by reducing the electrical signal bandwidth a trade-off can be reached between the impairment due to the bandwidth limitation and the advantage due to the crosstalk reduction. Figure 29 shows that for the optimal signal bandwidth of 16 GHz the single channel capacity is reduced by 10% but the 3-channel capacity improves of nearly 20%, in case of 35 dB OSNR. Further improvements are expected also by the optimization of the modulation amplitude and using some filtering at DSP level.

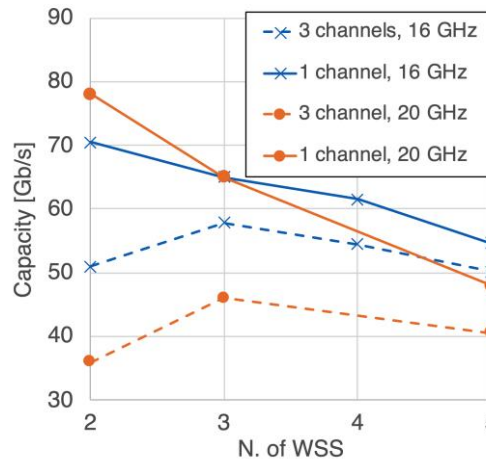


Figure 29 SSB DMT transmission capacities in 3-channel propagation vs number of crossed WSS for 35-dB OSNR: signal electrical bandwidth of 20 GHz (orange circles), signal electrical bandwidth of 16 GHz (blue crosses) 1 channel (continuous line), 3 channels (dashed line).

5.2 FEASIBILITY STUDY

Based on MS4 [MS4], we started the evaluation of the performance in terms of capacity as a function of the OSNR for connections representative of the network architecture characteristics. As so far defined in WP4, the filtering characteristics of HL4 nodes, and HL3 and HL1/2 nodes, for this set of simulations are considered as follows: the HL4 node filtering is represented by the AWG described and developed by VTT in D3.1 [D3.1], whereas HL3 and HL1/2 nodes include AWGs and WSSes as detailed in Section 3. The analysis of the performance in the multichannel linear regime allows the evaluation of a high number of nodes combinations covering a high percentile of actual links present in the sample network under study and needed for the study described in Section 2.1.3. In Section 5.2.1 we present a preliminary set of simulations for two link connections, while in Section 5.2.4 a more comprehensive analysis is performed to evaluate the performance of HL4-HL2 primary and secondary paths considering the distance and the number of hops of 90% of cases. On the other hand, NL simulations need to be performed on the actual link under study, thus due to computing complexity, in Section 5.2.2, we analyze the two worst cases where either the total covered distance or the number of hops is minimized as discussed in Section 2.1.3. Furthermore, in Section 5.2.3 the analysis is based on the experimental results of a representative HL4-HL2/1 multi-hop connection.

5.2.1 Analysis of sample connections based on MS4 network architecture definition

As previously discussed in the following, we consider the two connection cases:

- HL4-HL3 connection including 6 (mean) hops, where the HL4 node filtering is represented by the above mentioned 100-GHz AWG. For a preliminary assessment, we take into account just the node filtering effect. Future work will also address an OSNR evaluation due to the SOA presence. Actually, in this situation the signal passes through 14 100-GHz AWGs (one in the S-BVTx module, 12 in the 6 HL4 nodes and one at the S-BVRx) and 2 WSS (one for SSB modulation and one at the Rx side); results for the single channel single polarization are displayed in Table 7.
- HL1/2-HL1/2 connection including 2 hops or more, where the HL1/2 node filtering is represented by 4 AWGs and 2 WSSes. Actually, in this situation the signal passes through 6 100-GHz AWGs (one in the S-BVTx module, 4 in the first HL1/2 node and one in the S-BVRx) and 4 WSS (one for SSB modulation, 2 in the first HL1/2 node and one at the Rx side) results for the single channel single polarization are displayed in Table 7.



Table 7 SSB DMT capacity as a function of the OSNR for the HL4-HL3 connection (case a) and HL1/2-HL1/2 connection including 2 hops or more (case b).

Connection type	OSNR		
	40 dB	35 dB	30 dB
Case a)	83 Gb/s	75 Gb/s	56 Gb/s
Case b)	58 Gb/s	50 Gb/s	44 Gb/s

As in case of OSNR below 30 dB, the performance due to the node filtering effects is close to 50 Gb/s. These preliminary results evidenced the necessity to identify a few worst case scenarios, on which to evaluate the performance in NL regime and then to evaluate in the linear regime. This allows to identify the necessary OSNR, targeting HL4-HL2 primary and secondary paths, while considering the distance and the number of hops of 90% of the network cases, for three capacity rates as described in Section 2.1.3.

5.2.2 NL analysis of worst cases

The performance for the two worst cases described in Section 2.1.3 are evaluated in the NL regime in presence of 7 channels with 25 GHz spacing. In particular, as depicted in Figure 30, at the HL4 node level we have three propagating channels with 50-GHz spacing, at the first HL3 node four other 50-GHz spaced channels are added, shifted in frequency of ± 25 GHz, so that at the output of the first HL3 node we have 7 channels, 25-GHz spaced propagating in the path. The channel under test (CuT) is the central one and it is at 1550 nm.

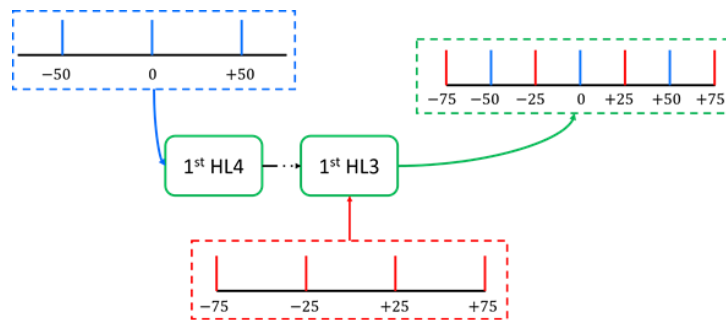


Figure 30 Signal channel spacing (in GHz) at the first HL4 node and at the first HL3 node.

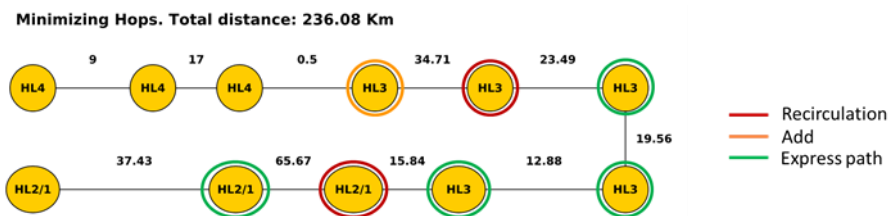


Figure 31 Minimizing hops setup with HL3 node functioning

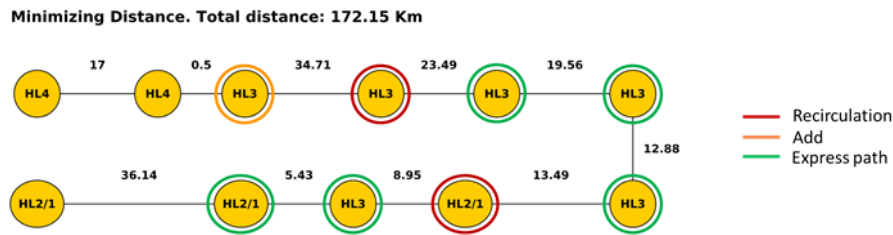


Figure 32 Minimizing distance setup with HL3 node functioning

All the channels have the same polarization, so also if we are taking into account a single polarization, we are actually overestimating the NL impairments. The transmitted signal is obtained by directly modulating an 18-GHz bandwidth VCSEL with the previously described 16-GHz SSB DMT signal; the bias current and the modulation amplitude are 9 mA and 10 mA, respectively, further DMT signal optimization can be obtained in case of wider VCSEL bandwidths. The channels propagate along SSMF fibre spans with 0.25 dB/km attenuation and 16 ps/nm·km dispersion at 1550 nm and impaired by self-phase modulation and cross-phase modulation. Erbium-doped fibre amplifiers (EDFAs) with a Noise Figure (NF) of 7 dB are employed to compensate for the transmission losses. For both the cases, several different scenarios have been considered. In a scenario the amplifiers have been placed at each node, while in the other(s) some spans have been rearranged considering a distance between two adjacent amplifiers around 35 km, where possible. The received power is set to 0 dBm, while the transmitted power is varied to obtain the best trade-off between OSNR and NL impairments. The coherent receiver, characterized by 25-GHz electrical bandwidth, exploits a 10-dBm per polarization Local Oscillator (LO) with 100-kHz linewidth. The DSP at the receiver provides CD compensation, digital synchronization, CP removal, sub-carriers phase recovery, demodulation, and error count. Chow’s BL algorithm is performed to evaluate the transmitted signal capacity [Chow95] when the target BER is set to 3.8×10^{-3} (corresponding to 7% overhead hard decision FEC limit).

The two worst cases are shown in Figure 31 and Figure 32, which recover Figure 6; although the two cases have been selected with different algorithms both present 10 hops, the “minimizing distance” one has a total path length of 172 km, while the “minimizing hops” of 236 km. As previously discussed, the HL4 nodes are constituted of two 50-GHz spaced flat-top AWGs, the HL3 and the HL2/1 nodes are composed of two 100-GHz bandwidth MUX and 1 WSS with 25-GHz channel spacing. As discussed in Section 3, the chosen node architectures and SDN central controller allow to efficiently manage the spectral resource. In particular here we make the hypothesis that at the first HL3 some channels will be added following the added-traffic path (as described in Section 3), while at the second HL3 the traffic will be re-organized by traversing the “recirculating path” (including the disaggregate/aggregate functionalities within the switching node) so that in the further HL3 hops the traffic will follow the “express traffic paths” until the first HL2 node, where another re-organization will take place through the “recirculating path”.

The network topology for the worst case scenario “minimizing distance” is shown in Figure 32. The first HL4 node provides for the multiplexing of the three 50-GHz spaced channels, along with SSB transmission. The first HL3 node adds the adjacent 4 channels, while from the second HL3 node the signal follows the previously described paths, recirculating in the second HL3 node and following the express path in the other HL3 nodes. In the first HL2/1 node the signal follows the recirculating path, while in the second, it follows the express path. The last HL2/1 node demultiplexes the signal, and selects the desired channel. Two different scenarios have been studied: in the first scenario the amplifiers have been placed after each span but the span of 0.5 km (every segment), and in the other scenario some spans have been aggregated (given segments). The aggregation of the spans has been achieved by considering 19.56 km and 12.88 km as a single span, and 13.49 km, 8.95 km, and 5.43 km as another single span. For both curves in Figure 33, the optimal optical power



representing a trade-off between OSNR and NL impairments is 1 dBm. Moreover, looking also at Table 8 a) and b) it can be noticed that the capacity increases when some of the spans are aggregated (given segments blue curve in the Figure 33), despite having a comparable value of OSNRs. The signal, in fact, faces a slightly higher attenuation, reducing the average span power, which lowers the impact of the non-linear effects. On the other hand, if we compare the obtained results with the performance of propagation in linear regime (around 54.2 Gb/s) we observe a capacity reduction due to the non-linear effects around 6%.

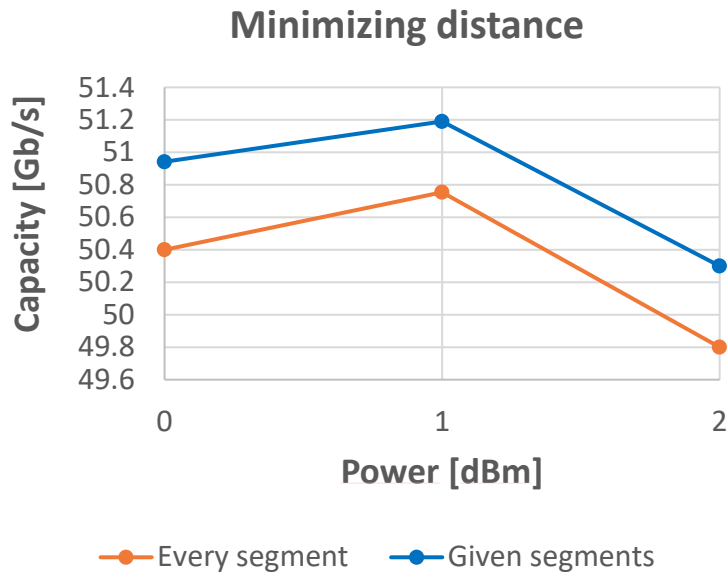


Figure 33 Transmitted capacity for minimizing distance case.

Table 8 SSB DMTO SNR and capacity as a function of the launched power for a) the OA in every span case and b) the OA in given span case.

a) OA in every span		
Input power [dBm]	OSNR [dB]	Capacity [Gb/s]
0	37.01	50.4
1	38.01	50.75
2	39.01	49.8

Linear propagation at 1 dBm:
54.13 Gb/s

b) OA in given spans		
Input power [dBm]	OSNR [dB]	Capacity [Gb/s]
0	37.19	50.9
1	38.19	51.19
2	39.19	50.3

Linear propagation at 1 dBm:
54.2 Gb/s

In the “minimizing hops” case, actually, we have a very similar situation as in the “minimizing distance” case with a longer overall path (Figure 31). We have thus evidenced four different simulation scenarios which are obtained by combining two choices: i) the aggregation or not of shorter spans (9 km and 17 km as a span, 23.49 km and 19.56 km as another single span, and 12.88 km, and 15.84 km as a further single span) ii) the split or not of the 65-km span. Figure 34 summarizes the results of the four simulations. Again, for all the four cases the optimal launch power is 1 dBm. The main difference in capacity performance arises from the 65-km span split in two separate amplified spans (35 km and 30.67 km) and, as can be seen in Table 9 c) and d), is due to an increase in the OSNR of 2 dB. Finally, if we compare these results with the performance obtained in the linear regime, we see that the NL effects lead to a reduction of the transmitted capacity of 11% in the case of 65-km span, and of 8.5% when the span is split. When the shorter spans are



aggregated, the OSNR and the transmitted capacities are comparable to the case of amplifiers installed at each node, both in case of a single 65-km long span and when the 65-km span is split.

It can be concluded that in case of similar number of hops of course the best performance is achieved when the overall path length is minimized, moreover for transmission distances up to around 150 km the NL effects reduce the linear propagation capacity around 5% even when considering co-polarized 25-GHz spaced channels.

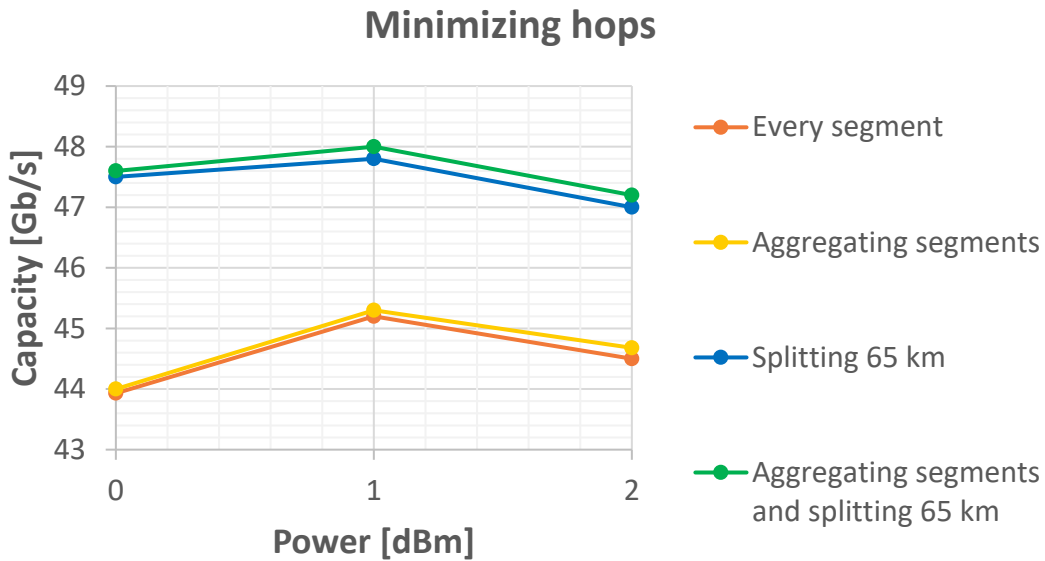


Figure 34 Transmitted capacity for minimizing hops case in four simulation scenarios.

Table 9 SSB DMTOSNR and capacity as a function of the launched power for a) the OA in every span case, b) the OA in given span splitting the 65-km span case, a) the OA in every span case and b) the OA in given span splitting the 65-km span case.

a) OA in every span		
Input power [dBm]	OSNR [dB]	Capacity [Gb/s]
0	34.45	43.93
1	35.45	45.2
2	36.45	44.5

Linear propagation at 1 dBm: 50.9 Gb/s

b) OA in given spans		
Input power [dBm]	OSNR [dB]	Capacity [Gb/s]
0	34.32	44
1	35.32	45.3
2	36.32	44.68

Linear propagation at 1 dBm: 50.8 Gb/s

c) OA in every span splitting 65 km		
Input power [dBm]	OSNR [dB]	Capacity [Gb/s]
0	36.32	47.5
1	37.32	47.8
2	38.32	47

Linear propagation at 1 dBm: 52.2 Gb/s

d) OA in given spans splitting 65 km		
Input power [dBm]	OSNR [dB]	Capacity [Gb/s]
0	36.12	47.6
1	37.12	48
2	38.12	47.2

Linear propagation at 1 dBm: 52 Gb/s



5.2.3 PASSION photonic system architecture assessment for multi-hop HL4-HL2/1 connectivity enabling IP-offloading

According to the case analysis in Sec. 2.1, and to the related findings in terms of path length minimizing the hops, we have performed an experimental assessment (joint activity with WP5) in order to assess the feasibility of the PASSION approach and to derive important considerations related to it. Here, we describe the developed proof of concept and report the main results leading to relevant conclusions and take-over messages to continue working on the PASSION photonic system architecture optimization and in view of the work within WP5.

The SDN-enabled photonic system architecture has been experimentally assessed across multiple HL, through up to 6 aggregation nodes and 160 km long path, including the ADRENALINE testbed network (4-node fixed/flexi-grid mesh network with amplified links) and a 25km 19-core MCF with fan-in and fan-out [Sva20]. In fact, based on the analysis in Sec. 2.1.3 the path length from HL4 to HL2/1 (minimizing the hop number) in the worst case can reach about 150km, while in average the number of hops is < 7.

A single flow transceiver has been analyzed adopting a VERTILAS VCSEL with bandwidth limited to 10 GHz (due to the packaging and evaluation board adopted). It operates at 1545.32nm (194.00THz), which corresponds to a nominal central frequency $n=144$ and represents VCSEL-6, within subMOD-2 of MOD-1, as indicated in the inset at the left of Figure 35. For the S-BVT Rx, both DD and CO-Rx module options have been considered and compared, in order to validate the choice of adopting CRM as PASSION solution dealing with the targeted MAN and use cases of interest and also to explore the possibility of adopting an even more cost-effective Rx design. The DD module consists of a PIN diode with 20GHz bandwidth and includes a transimpedance amplifier (TIA); the considered CO-Rx has discrete components up to 40GHz bandwidth (due to laboratory availability at the time of the experiment) and includes a tunable LO.

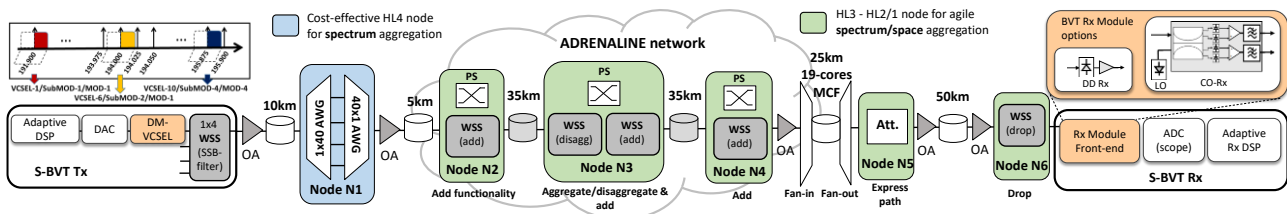


Figure 35. Experimental set-up for PASSION system proof of concept [Sva20].

Up to 6 WSSs (emulating HL3 and HL2/1 nodes) with 50GHz granularity and two 100GHz AWGs (emulating HL4 node) are traversed. The WSS at the Tx is for SSB filtering. The HL3 and HL2/1 WSS-based filtering stages implement the different functionalities described in Sec. 3: add functionality, aggregate/disaggregate functionality (to spectrally combine the considered flow with other flows at the HL3 node, also referred to as “recirculation” / “recirculating path” in previous Section 5.2.2). In addition to the photonic switches at the ADRENALINE nodes, variable and fixed attenuators have been considered in the set-up in order to emulate the PASSION photonic switch modules present at HL3 and HL2/1 nodes (see Sec. 3). Particularly, a 2-dB attenuator (Att.) after the 19-core MCF emulates the express path at N5 node. In the last HL2/1 node, a WSS is considered for dropping the traffic towards the S-BVT Rx. The 35km standard single-mode fiber (SSMF) links of the ADRENALINE network are pre-amplified, while optical amplifiers (OAs) are indicated in Figure 35.

The obtained results show that DD is more affected by the OSNR degradation and path length increase, while CO-Rx allows supporting more than 30 Gb/s in back-to-back (B2B) and above 20 Gb/s capacity over the HL4-HL2/1 multi-hop path connection even with 10GHz VCSEL [Sva20].



Furthermore, it has been confirmed that integrated coherent receiver outperforms both DD and CO-Rx based on discrete components. Thus, we can conclude that the achieved results are really promising. In fact, adopting programmable photonic transceivers based on >18GHz VCSELs and integrated CO-Rx, the support of higher capacities is expected. A theoretical model has been also developed for the PASSION system and compared with the experimental results, showing an upper bound for the expected results [Fab20B]. Further scalability can be obtained exploiting the spatial dimension.

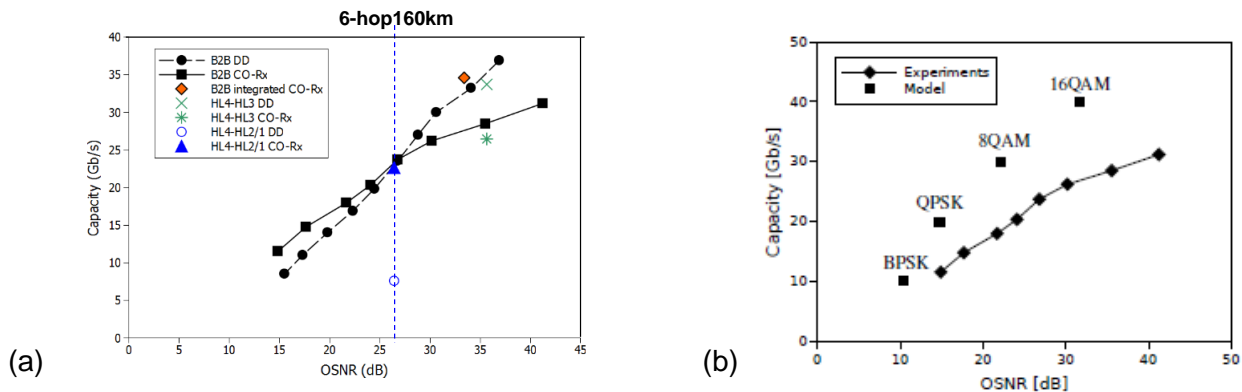


Figure 36. (a) Experimental results. The case of 6-hop and 160km for DD and CO-Rx is evidenced; 2-hop and 15km case for a HL4-HL3 connection is also reported. (b) Comparison of experimental B2B results and theoretical model for CO-Rx.

5.2.4 OSNR requirements for the support of 90% HL4-HL2/1 primary and secondary paths

In Sec. 2.1.3, after the identification of the two worst case paths already analyzed in the previous section, it has been evident that it is important to evaluate the path characteristics in terms of total path length and of number of hops of the 90% HL4-HL2 primary and secondary paths. In particular it has been found that when adopting a “minimizing hop” strategy to define the path, the more stringent requirement is represented by the 11 hops needed to support the 90% of HL4-HL2 secondary paths with a path length of around 115 km. Moreover, in Sec. 2.1.3 three target capacities have been identified as paramount for the PASSION approach, namely 50 Gb/s, 40 Gb/s and 25 Gb/s. Here with the approach described in Section 5.1.3 we determine the OSNR which is needed to support the above mentioned paths granting those capacities; it has been demonstrated in Section 5.2.2, in fact, that in case of path length shorter than 150 km the obtained accuracy almost matches the complete NL approach one even with co-polarized and fully loaded channels.

The analysis is performed by taking into account the channel occupancy (i.e. with a complete 7-channel 25-GHz spacing grid) by co-polarized DMT modulated signals as shown in Figure 30. In particular, as evidenced in Section 5.1.3, in order to limit the spectrum broadening, the 18-GHz bandwidth VCSELs are directly modulated with a 16-GHz DSB DMT signal; the bias and modulation-amplitude currents are 9 mA and 10 mA respectively. The transmitted power is 1 dBm, as it has been previously demonstrated (Section 5.2.2) to be the optimal power. At the HL4 level the 50-GHz spaced channels are modulated with a DSB signal, while the first HL3 node performs the SSB filtering and it adds the adjacent channels. In all the HL3 nodes but the first and the last one (where the desired channel is selected) the signal is supposed to follow the recirculating path; this, as previously discussed, represents a very worst case condition as very likely after the second HL3 node the channels will be arranged to efficiently manage the spectral resource and use the express-path in the following HL3 nodes. The signal propagates along SSMF fibre spans impaired only by linear effects (0.25 dB/km attenuation and 16 ps/nm·km CD at 1550 nm). The optical noise arising from the presence of EDFAs is accounted for by varying the transmission OSNR. The signal is



coherently detected with a CO-Rx characterized by 25-GHz bandwidth and exploiting a 10-dBm LO with 100-kHz linewidth. The received power is 0 dBm; the receiver DSP performs CD compensation, digital synchronization, CP removal, sub-carriers phase recovery, demodulation, and error count. The target BER is set to 3.8×10^{-3} (corresponding to 7% overhead hard decision FEC limit) to evaluate the transmitted capacity with the Chow’s algorithm [Chow95].

Table 10, Table 11 and Table 12 summarize the obtained minimum OSNRs to achieve the target capacity of 50 Gb/s, 40 Gb/s and 25 Gb/s respectively. As previously recovered, in order to support the 90% of HL4-HL2 secondary paths the maximum number of crossed nodes is 11, the Tables thus include all the combinations of HL4 and HL3 nodes to achieve a total number of 11 nodes, whereas the grey cells indicate that the sum between the numbers of HL4 and HL3 nodes exceeds 11.

Table 10 Minimum OSNR [dB] to target 50 Gb/s as a function of the number of HL4 and HL3 nodes.

OSNR requirements for 50 Gb/s target capacity							
		Number of HL3 nodes					
		1	2	3	4	5	6
Number of HL4 nodes	0	32.4	35.6	34	35.1	36.2	38.4
	1	32.2	35.4	34	35	36	38.2
	2	32	35.4	34	35	36	38.2
	3	32	35.2	33.8	35	36	38.2
	4	32	35.2	33.8	34.8	35.8	38
	5	31.8	35	33.6	34.8	35.8	38
	6	31.8	35	33.6	34.6	35.7	
	7	31.8	34.8	33.5	34.6		
	8	31.6	34.8	33.5			
	9	31.6	34.6				
	10	31.5					

Table 11 Minimum OSNR [dB] to target 40 Gb/s as a function of the number of HL4 and HL3 nodes.

OSNR requirements for 40 Gb/s target capacity												
			Number of HL3 nodes									
			1	2	3	4	5	6	7	8	9	10
Number of HL4 nodes	0	28	31	29.7	30.5	31.4	32.2	33.3	35.2	37.2	46	
	1	27.5	30.8	29.5	30.3	31.2	31.9	33	35	37	46	
	2	27.3	30.6	29.3	30.3	31	31.7	32.8	34.8	37		
	3	27	30.4	29.1	30.1	30.8	31.5	32.8	34.7			
	4	26.8	30.1	29	30.1	30.8	31.5	32.6				
	5	26.6	29.9	28.8	29.9	30.6	31.2					
	6	26.4	29.7	28.8	29.7	30.6						
	7	26.3	29.5	28.7	29.7							
	8	26.3	29.2	28.7								
	9	26.1	28.8									
	10	26										



Table 12 Minimum OSNR [dB] to target 25 Gb/s as a function of the number of HL4 and HL3 nodes.

ONSR requirements for 25 Gb/s target capacity												
		Number of HL3 nodes										
		1	2	3	4	5	6	7	8	9	10	
Number of HL4 nodes	0	23.3	25.3	23.4	23.5	24.6	25.2	26	26.3	26.8	27	
	1	22.5	24.8	23.1	23.4	24.2	24.8	25.5	25.8	26.3	26.5	
	2	22.2	24.2	23	23.3	24	24.6	25.3	25.7	26.3		
	3	21.8	23.8	22.5	22.9	23.8	24.4	25.2	25.6			
	4	21.6	23.5	22.2	22.8	23.6	24.3	25				
	5	21.3	23.2	22	22.6	23.4	24.3					
	6	21	23	21.8	22.6	23.4						
	7	20.8	22.8	21.5	22.5							
	8	20.6	22.6	21.3								
	9	20.4	22.4									
	10	20.2										

Table 10 shows that in the case of 50 Gb/s target capacity, not more than 6 HL3 nodes can be supported, even without the presence of optical noise. A 10- HL_3 nodes path requires an OSNR level comparable to the absence of optical noise even for 40 Gb/s target capacity (Table 11). Almost 20-dB lower OSNRs are otherwise required in case of 25 Gb/s capacity (Table 12). The previous tables highlight some important results. As expected, the impact of increasing the number of HL_3 nodes is higher in terms of requested OSNR with respect to the increase of HL_4 node number, as at each HL_3 node the signal is subject to 2 more 25-GHz WSS filtering, the equivalent filter tightening due to the filter cascading causes portions of the signal to be filtered out, severely impairing the performance. In the case of 2 HL_3 nodes, no matter the number of HL_4 nodes, the required OSNR is higher than in the case of 3 HL_3 nodes. This is due to a spurious cross-talk component from the adjacent channel at -25 GHz from the CuT, which lowers the SNR around 8.5 GHz, as shown in Figure 37. On the contrary, at the first HL_3 node there are only 50 GHz spaced channels and after the second HL_3 node the filter tightening due to filter cascading actually removes the spurious component (Figure 37 right).

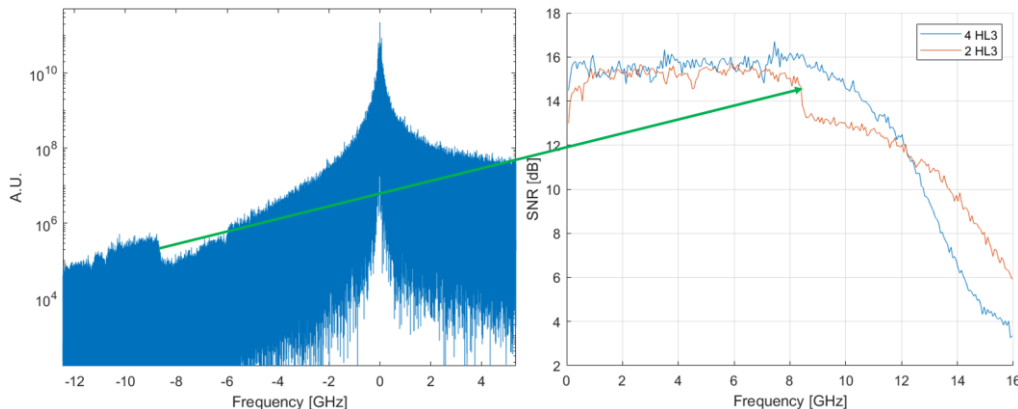


Figure 37 Spurious component affecting the SNR for 2 HL_3 nodes (left) SNR comparison for 2 and 4 HL_3 nodes.

Looking at the first column of each Table, it can be noticed that when increasing the number of HL_4 nodes, the required OSNR decreases. This is because the filter tightening due to filter cascading of



a high number of HL4 nodes acts as a WSS performing SSB, as can be seen in Figure 38 and in Figure 39, where a comparison of the spectrum at the transmitter and after 10 HL4 nodes is shown.

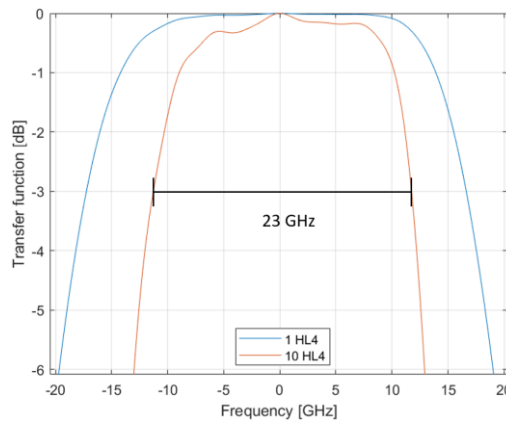


Figure 38: Tightening effect due to 1 to 10 HL4 filtering cascading.

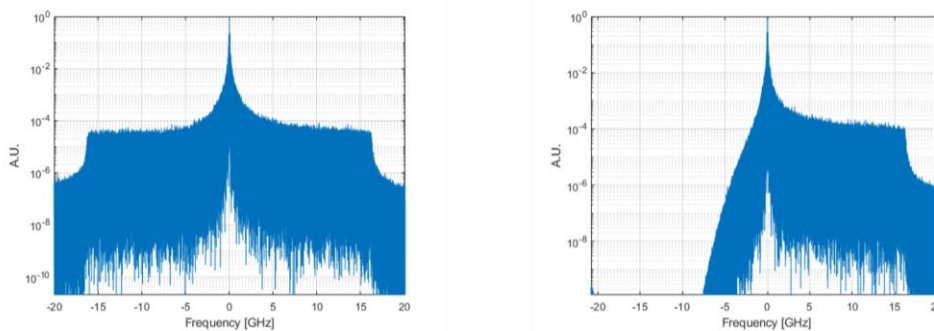


Figure 39: Spectra of the transmitted channel (left) and after 10 HL4 nodes (right)

The results presented in the previous Tables can be exploited to determine which capacity can be supported by the different HL4-HL2 links, by knowing the span lengths between consecutive nodes/amplifiers. Further ongoing investigations include the evaluation of the impact of the presence of SOAs in the nodes and the introduction of a correction mechanism in the linear model to take into account the impact of NL in DMT based transmission [Pog15].

6 CONCLUSIONS

This deliverable provides the PASSION node and transceiver architectures defined in T2.3. The programmable photonic system and subsystem architectures, including the S-BVT and the switching node as main network elements, have been carefully designed to address the targeted use cases, taking into account the challenging requirements in terms of capacity and paths to be supported. Programmability and control aspects, as well as the advances of the technology solutions developed in WP3 and WP4, have allowed a suitable and efficient modular architecture design towards a consolidated architecture and further integration and experimental validation in WP5.

The suitable modularity, as key feature for the node and transceiver composition and scalability, has been defined, fostering a pay-as-you-grow model and/or license-based element activation, in view of the network expansion/upgrade. Thus, the system or a specific node/transceiver can grow-as-needed to achieve the target capacity/flexibility, also according to the evolution of the network.



In particular, among the identified use case list of scenarios where to exploit PASSION solutions, use cases #1 and #3 are considered the most challenging and attractive to be addressed. Thus, they have been further analyzed in order to derive the requirements and scenarios to be analyzed from the technological and architectural viewpoints. Also, use case #6 on C-RAN support has been developed in more detail, identifying the advantages of adopting S-BVT and PASSION architecture to adapt the transmission capacity to the fronthaul (HL5-HL4) or midhaul traffic (HL4-HL2).

Suitable node architecture and granularity for the different HLs have been defined, taking into account the technological advancements and progresses in the switching elements. A more cost-effective design at HL4 handling only the spectral dimension with 50GHz granularity, adopting AWGs and wavelength blockers, is considered. At HL3 and HL2/1 WSS-based nodes with advanced functionalities and finer granularity (25GHz), are adopted to enable the management of both spectral and spatial dimensions, by means of photonic switch, add/drop WSS and MCS.

Both S-BVT transmitter and CRM receiver modules have been studied, designed considering alternative options to further confirm that PASSION approach is promising. Densely integrated direct multicarrier modulated VCSELs (optimized for high bandwidth modulation within the C-band) and integrated coherent detection with tunable LO are the preferred choices for achieving the targeted goals with a modular approach. The fundamental module at the Tx integrating 40 VCSELs on a SOI-chip and providing up to 2Tb/s is the transceiver architecture adopted at HL4 nodes and to be used for composing fully equipped S-BVT at higher HL nodes. Exploiting spectral dimension up to 8Tb/s capacity is supported, with polarization up to 16Tb/s, and in the spatial domain, using bundle of fibers or MCFs >100Tb/s capacities are obtained, respectively. This makes the proposed solution promising to target Tb/s MAN connections when combined with CRM.

To this extent, feasibility study and impairment tolerance assessment have been performed based on a PASSION simulation tool and numerical analysis supported by experimental measurements. Linear and non-linear propagation, VCSEL characteristics, optical filtering effects, CD, cross-talk from adjacent channels have been considered. Also, a theoretical model has been developed for the PASSION approach, as a benchmark for the expected performance. Based on the identified use cases, the most challenging scenarios, particularly the one envisioning IP offloading at HL3, have been numerically and experimentally analyzed to assess and validate the designed architectures and towards their improvement/optimization. Extensive simulations have been performed to obtain the optical signal to noise ratio (OSNR) requirements for given target capacities (50 Gb/s, 40 Gb/s, 25 Gb/s) considering the targeted most challenging use cases.

Flexibility, dynamicity and adaptation to the available resources and requested traffic demands are addressed with the support of SDN-programmability as defined in D2.2. An efficient management of spectral and spatial resources, including different network elements, granularities and functionalities, has been considered to comply with the stringent identified requirements. OPEX and CAPEX will be further taken into account in WP2's final deliverable D2.4, where an in-depth techno-economic analysis of PASSION technology/approach based on the most relevant use cases will be performed.

The PASSION node and transceiver architectures, with all the findings, results and specificities reported in this document provide relevant material and guidelines for the work to be performed in WP5. Further refinement/optimization of the final design can be performed within WP2, based on next advances on the work developed within WP3, WP4 and with further feedback of the activities within WP5.



7 REFERENCES

- [D2.1] "Defintition of the use cases and requirements for network, systems and subsystems", PASSION D2.1, Septemeber 2018.
- [D2.2] "Overall network architecture and control aspects definition, PASSION Project D2.2, January 2020.
- [D3.1] Design of the Tx module architecture and interfaces, PASSION Project D3.1, April 2018.
- [D3.2] "First testing of directly modulated VCSELs with selected drivers", PASSION Project D3.2, May 2018.
- [D4.1] "Circuitry and technology matching to the path functionality in the optical node", PASSION Project D4.1, March 2018.
- [D4.2] "First generation of hardware efficient modular coherent receivers," Feb. 2019.
- [D4.6] "Second generation of hardware efficient modular coherent receivers," Feb. 2020.
- [MS4] "Preliminary definition of the network architecture," PASSION Project MS4, Nov 2018.
- [MS6] "Preliminary definition of the node and transceiver architecture," PASSION Project MS6, Jan. 2020.
- [Bha19] S. Bhat, M. Harjanne, F. Sun, M. Cerchi, M. Kapulainen, A. Hokkanen, G Delrosso, T. Alto, "Low Loss Devices fabricated on the Open Access 3 μm SOI Waveguide Platform at VTT" in Proc. *European Conference on Integrated Optics* (2019) Ghent, Belgium.
- [Bof20] P. Boffi, et al., "Multi-Tb/s sustainable MAN scenario enabled by VCSEL-based innovative technological solutions," Proc. SPIE 11308, Metro and Data Center Optical Networks and Short-Reach Links III, 113080G, Jan. 2020.
- [Chow95] P. S. Chow, J.M. Cioffi, J.A.C. Bingham "A practical discrete multitone transceiver loading algorithm for data transmission over spectrally shaped channels," IEEE Trans. on Comm., 43, 773-775 (1995).
- [Fab20A] Josep M. Fabrega et al., "Programmable Transmission Systems using Coherent Detection enabling Multi-Tb/s Interfaces for IT-communications Convergence in Optical Networks," Proc. SPIE 11308, Metro and Data Center Optical Networks and Short-Reach Links III, Jan 2020.
- [Fab20B] Josep M. Fabrega et al., "Cost-effective Coherent Systems for Metropolitan Networks," in Proc. ONDM 2020.
- [HHI] <https://www.hhi.fraunhofer.de/en/departments/pc/research-groups/photonic-inp-foundry.html>
- [ITU] Recommendation ITU-T G694.1, "Spectral grids for WDM applications: DWDM frequency grid," (2012).
- [Lar19] D. Larrabeiti, J. Fernández-Palacios, G. Otero, M. Svaluto Moreolo, J. M. Fabrega, R. Martínez, P. Reviriego, V. López, "All-Optical Paths across Multiple Hierarchical Levels in Large Metropolitan Area Networks," in Proc. ACP 2019.
- [Lar20] D. Larrabeiti, G. Otero-Pérez, J. A. Hernández, P. Reviriego, J. Fernández-Palacios, V. López, M. Svaluto Moreolo, R. Martínez, J. M. Fabrega "Tradeoffs in optical packet and circuit transport of fronthaul traffic: the time for SBVTs?" in proc. ONDM2020, May 2020.



- [Mar19] R. Martínez et al., "Proof-of-Concept validation of SDN-controlled VCSEL-based S-BVTs in flexi-grid optical metro networks," in Proc. OFC 2019, San Diego, CA (USA), March 2019.
- [Mar20] R. Martínez, et al., "Experimental evaluation of an on-line RSA algorithm for SDN controlled optical metro network with VCSEL-based S-BVTs", in Proc. ONDM 2020.
- [Mue11] Mueller M., et al., "1550 nm highspeed short-cavity VCSELs," IEEE J. Sel. Topics Quantum Electron., vol. 17, no. 5, pp. 1158–1166, (2011).
- [Pog15] P. Poggiolini, G. Bosco, A. Carena, V. Curri, Y. Jiang, and F. Forghieri, "A simple and effective closed-form GN model correction formula accounting for signal non-Gaussian distribution," J. Lightw. Technol., 33, 2, 459–473, 2015.
- [Pulik11] C. Pulikkaseril, L. A. Stewart, M. A. F. Roelens, G. W. Baxter, S. Poole, and S. Frisken, "Spectral modeling of channel band shapes in wavelength selective switches," Opt. Express 19, 8458-8470 (2011).
- [Rap18] M. Rapisarda, et al. "Impact of Chirp in High-Capacity Optical Metro Networks Employing Directly-Modulated VCSELs" Photonics, 5, 51, 1-11 (2018).
- [Sva16] M. Svaluto Moreolo et al., "SDN-Enabled Sliceable BVT Based on Multicarrier Technology for Multiflow Rate/Distance and Grid Adaptation," IEEE/OSA J. Lightwave Technol., 34, 6, 1516-1522 (2016).
- [Sva18] M. Svaluto Moreolo, J. M. Fabrega, L. Nadal, R. Martínez, R. Casellas, "Synergy of photonic technologies and software-defined networking in the hyperconnectivity era," Submitted to IEEE/OSA J. Lightwave Technol. Special Issue on Photonic Networks and Devices, Dec. 2018.
- [Sva19A] M. Svaluto Moreolo et al., "VCSEL-based sliceable bandwidth/bitrate variable transceivers," SPIE-PWO, San Francisco, CA (USA), Feb. 2019.
- [Sva19B] M. Svaluto Moreolo et al., "Programmable VCSEL-based Transceivers for Multi-terabit Capacity Networking," CLEO 2019, San Jose, CA (USA), May 2019.
- [Sva19C] M. Svaluto Moreolo, R. Martínez, L. Nadal, J. M. Fabrega, N. Tessema, N. Calabretta, R. Stabile, P. Parolari, A. Gatto, P. Boffi, G. Otero, D. Larrabeiti, J. A. Hernandez, P. Reviriego, J. P. Fernández-Palacios, V. López, G. Delrosso, C. Neumeyr, K. Solis-Trapala, G. Parladori, G. Gasparini, "Spectrum/Space Switching and Multi-Terabit Transmission in Agile Optical Metro Networks," in Proc. OECC/PSC, July 2019, Fukuoka, Japan.
- [Sva20] M. Svaluto Moreolo, J. M. Fabrega, L. Nadal, R. Martínez, R. Casellas, J. Vílchez, R. Muñoz, R. Vilalta, A. Gatto, P. Parolari, P. Boffi, C. Neumeyr, D. Larrabeiti, G. Otero, J. P. Fernández-Palacios, "Experimental Assessment of a Programmable VCSEL-based Photonic System Architecture over a Multi-hop Path with 19-Core MCF for Future Agile Tb/s Metro Networks," in Proc. OFC 2020.
- [Xie15] C. Xie, et al., "Single-VCSEL 100-Gb/s short-reach system using discrete multi-tone modulation and direct detection", Proc. OFC 2015, Los Angeles, CA (USA), pp. 1-3, 2015.



8 ACRONYMS

AIN	Aluminium Nitride
AWG	Arrayed Waveguide Grating
BL	Bit Loading
BTJ	Buried Tunnel Junction
BVT	Bandwidth-Variable Transceiver
CAPEX	Capital Expenditure
CD	Chromatic Dispersion
CDN	Content Delivery Network
CO-Rx	Coherent Receiver
CPWG	Coupled coplanar waveguide
CRM	Coherent Receiver Module
CSI	Channel State Information
DBR	Distributed Bragg Reflector
DMT	Discrete Multitone
DRoF	Digitized radio over fiber
DSB	Dual Sideband
DSP	Digital Signal Processing
DM	Direct Modulation
EDFA	Erbium-Doped Fiber Amplifier
E/O	electro/optical
FEC	Forwarding Error Correction
FSR	Free Spectral Range
HLn	Hierarchy Level n
InP	Indium Phosphide
IPTV	IP Television
MA	Margin Adaptive
MAN	Metropolitan Area Network
MCM	Multicarrier modulation
MCS	Multicast switch
MCF	Multicore Fiber
MQW	Multi Quantum Well
NL	Nonlinear
LO	Local Oscillator
OA	Optical Amplifier
OFDM	Orthogonal Frequency Division Multiplexing
OPEX	Operational Expenditure
OSA	Optical Subassembly
OSNR	Optical Signal-to-Noise Ratio
PD	Photodiode
PDM	Polarization-Division Multiplexing
PIC	Photonics Integrated Chip
PL	Power Loading
PMF	Polarization-Maintaining Fiber
PRBS	Polarization Rotating Beam Splitter
PSM	Photonic Switching Module
QoT	Quality of transmission
RA	Rate Adaptive
RSA	Routing and Spectrum Assignment
Rx	Receiver



RWA	Routing and Wavelength Assignment
S-BVT Rx	S-BVT Receiver
S-BVT	Sliceable-Bandwidth-Variable Transceiver
S-BVT Tx	S-BVT Transmitter
SC	Short-Cavity
SDM	Space-Division Multiplexing
SDN	Software Defined Networking
SMSR	Side Mode Suppression Ratio
SNR	Signal-to-Noise Ratio
SOA	Semiconductor Optical Amplifier
SOI	Silicon On Insulator
SOP	state of polarization
SSB	Single Sideband
SSC	Spot size converter
SSMF	Standard Single-Mode Fiber
SWT	Switch
TEC	Thermoelectric cooler
TIA	Transimpedance Amplifier
Tx	Transmitter
VCSEL	Vertical-Cavity Surface-Emitting Laser
VPN	Virtual Private Network
WDM	Wavelength-Division Multiplexing
WSS	Wavelength Selective Switch
YANG	Yet Another Next Generation